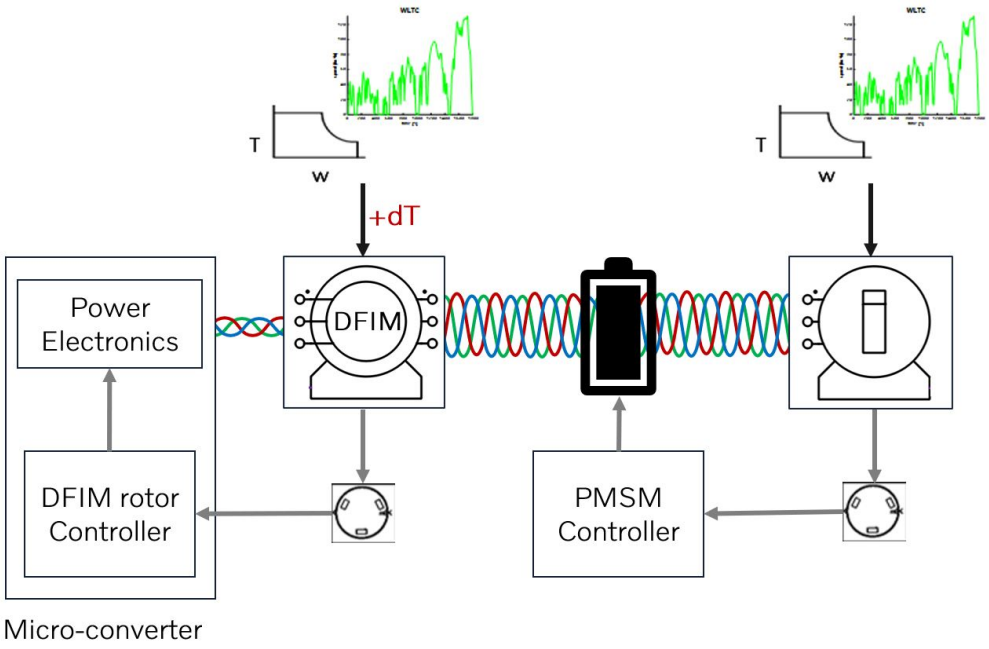

Double Fed Induction Machine for All-wheel-drive Application in Electric Vehicles

Master's thesis in Electrical Engineering

Shashank G. Shanbhag & Sri Harsha Dannana

DEPARTMENT OF ELECTRICAL ENGINEERING
Chalmers University of Technology
Gothenburg, Sweden 2024
www.chalmers.se

Master's thesis 2024

Double fed Induction Machine for All-wheel-drive Application in Electric Vehicles

Shashank G. Shanbhag & Sri Harsha Dannana

CHALMERS

Department of Electrical Engineering
Division of Electric Power Engineering
Chalmers University of Technology
Gothenburg, Sweden 2024

Double-fed induction machine for all-wheel-drive application in electric vehicles
Shashank G. Shanbhag & Sri Harsha Dannana

Supervisor: Aditya Pratap Singh, Volvo Car Corporation & Jonas Forssell, Volvo Car Corporation
Examiner: Dr. Yujing Liu, Department of Electrical Engineering

Master's Thesis 2024
Department of Electrical Engineering
Division of Electric Power Engineering
Chalmers University of Technology
SE-412 96 Gothenburg
Telephone +46 31 772 1000

Cover: Double fed induction machine all-wheel-drive system layout.

Gothenburg, Sweden 2024

Abstract

The transition to electric vehicles (EVs) demands innovative drivetrain solutions that maximize performance, reliability and reduces complexity and cost. This thesis deals with the modelling, novel strategy for controlling, and analysis of double-fed induction machines (DFIM) for an all-wheel-drive scenario in electric vehicles and the integration of double-fed induction machines (DFIM) in electric all-wheel-drive (AWD) systems, aiming to maintain performance comparable to conventional systems using induction machines (IM) and permanent magnet synchronous machines (PMSM). The research addresses the challenge of reducing overall components in an electric AWD system by replacing the IM+PMSM combination with a DFIM+PMSM setup, utilising a single, compact micro-converter at the DFIM rotor, and controlling the PMSM and DFIM stator through a PMSM controller.

The study begins by examining the fundamental principles of DFIMs, highlighting their dual stator and rotor winding configuration which allows for variable frequency control through power electronics. This unique characteristic facilitates bidirectional power flow and regenerative braking, key advantages for EV applications. The thesis then discusses the working of DFIMs into AWD systems, focusing on the requirements of power between the rotor and stator of the DFIM in order to provide deeper understanding into coordination of torque to improve handling and performance.

Simulation models and experimental setups are utilized to analyse the performance of DFIM-based AWD systems under different driving conditions. Key performance indicators such as efficiency, response time, traction control, and energy consumption are evaluated and compared with traditional AWDs with induction motor as the front (auxiliary) drive and permanent magnet synchronous motor(PMSM) at the rear (primary) drive. The results indicate that DFIMs offer enhanced efficiency and torque control, while reducing the power electronics requirement significantly. This is achieved by powering both the DFIM stator and PMSM stator using the PMSM controller and exciting the DFIM rotor using a micro converter. Results demonstrated that the DFIM consumes minimal rotor power (up to 6 kW) in a 215 kW machine, suggesting its feasibility for AWD applications. The DFIM can operate in tandem with the PMSM in a 60-40 or 80-20 torque split, reducing losses associated with disengaging the DFIM.

Furthermore, the thesis addresses the challenges of implementing DFIMs in AWD systems, including control complexity, and cost considerations. Estimation of DFIM machine parameters, robust control algorithms, and cost-effective drivetrain options are proposed as potential solutions to these challenges.

In conclusion, DFIMs present a promising alternative for AWD systems in electric vehicles, offering significant benefits in terms of efficiency, performance, and control. The insights gained from this study could pave the way for the development of more advanced and efficient electric drivetrains, contributing to the broader adoption of electric vehicles and the advancement of sustainable transportation technologies.

Key terms: double-fed induction machine, all-wheel-drive, variable stator voltage, independent rotor controller, field-oriented control, energy efficiency

Acknowledgements

We would like to express our sincere gratitude to the Department of Strategy & Program Execution at Volvo Car Corporation, Gothenburg, Sweden, for providing outstanding facilities and entrusting us with the opportunity to pursue our master's thesis. The experience of working at Volvo Car Corporation has been both highly educational and profoundly rewarding.

We are sincerely grateful to our supervisor, Aditya Pratap Singh, for his unwavering support and motivation. His mentorship and trust in us made this journey both smooth and rewarding.

We also wish to thank Prof. Yujing Liu, our academic examiner, for his invaluable guidance throughout our thesis and master's studies at Chalmers University of Technology. Our thanks also go to the Department of Electrical Engineering, particularly the Division of Electric Power Engineering and Department of Mechanics and Maritime Sciences for the learning opportunities provided.

Lastly, we express our heartfelt thanks to Jonas Forssell, Anders Bergqvist, and Joachim Härsjö for their insightful guidance and continuous support during our thesis.

Shashank G. Shanbhag, Gothenburg, August 2024
Sri Harsha Dannana, Gothenburg, August 2024

Contents

List of Tables

List of Figures

Acronyms

AC Alternating Current

AWD All-Wheel-Drive

DC Direct Current

DFIG Double Fed Induction Generator

DFIM Double Fed Induction Machine

DTC Direct Torque Control

EV Electric Vehicle

FOC Field Oriented Control

FWD Front-Wheel-Drive

HEV Hybrid Electric Vehicle

IGBT Insulated-Gate Bipolar Transistor

IM Induction Machine

MOSFET Metal-Oxide-Semiconductor Field-Effect Transistor

MTPA Maximum Torque Per Ampere

PI Proportional-Integrator controller

PLL Phase Locked Loop

PMSM Permanent Magnet Synchronous Machine

RPM Revolutions Per Minute

RRF Rotor Reference Frame

RWD Rear-Wheel-Drive

SRIM Slip Ring Induction Machine

VSTS Variable Speed Traction Systems

WLTC World-wide harmonized Light duty vehicle Testing Cycle

WRIM Wound Rotor Induction Machine

Nomenclature

Abbreviations

i^*_{Rd}	reference current in Γ model, in d-axis
i^*_{Rq}	reference current in Γ model, in q-axis
$L^{'}_{r\lambda}$	rotor leakage inductance
$L_{r\lambda}$	rotor leakage inductance w.r.t the stator
$L_{s\lambda}$	stator leakage inductance
B	friction coefficient
B_a	active damping
f_s	stator frequency, synchronous frequency
I_{rd}	rotor current, in d-axis
I_{rq}	rotor current, in q-axis
i_R	rotor current in Γ-model
i_r	rotor current
I_{sd}	stator current, in d-axis
I_{sq}	stator current, in q-axis
i_s	stator current
J	inertia
k_i	integral constant
k_p	proportional constant
k_w	anti-windup factor
L_σ	Leakage inductance in Γ model
L_m	Magnetising inductance
n_p	number of pole pairs
N_r	number of winding turns on rotor
n_r	mechanical speed of rotor
n_{syn}	mechanical synchronous speed

N_s	number of winding turns on stator
P	power
P_m	mechanical power
P_r	rotor power
P_s	stator power
$R_r^{'}$	rotor resistance
R_R	rotor resistance in Γ-model
R_r	rotor resistance w.r.t the stator
R_s	stator resistance
s	slip
T	mechanical torque
T_e	electrical torque
T_L	load torque
u	turns ratio
V	voltage
V_{abc}	three phase voltage
v_R	rotor voltage in Γ-model
v_r	rotor voltage
v_s	stator voltage

Symbols

Ψ_R	rotor flux in Γ-model
Ψ_r	rotor flux
Ψ_s	stator flux
Δ	difference, drop
η_{DFIM}	DFIM efficiency
$\hat{\psi}_s$	estimated stator flux
Ω_r	mechanical angular speed of rotor
ω_r	angular frequency of rotor voltage, electrical speed of stator
ω_{slip}	slip frequency
ω_s	angular frequency of stator voltage, electrical speed of stator
θ_{slip}	electrical slip angle position

Subscripts

λ	leakage
σ	leakage inductance in Γ model
abc	three-phase system
d	direct

DFIM	double fed induction machine
e	electric
L	load
m	magnetising
p	pole pairs
q	quadrature
r	rotor
s	stator
slip	electrical slip
syn	synchronous

Superscripts

’	referred to the rotor
*	reference
∧	estimated, peak/maximum value, amplitude

1

Introduction

Double-fed induction machines (DFIM) are widely used in wind turbines and are also being researched for application in marine drivetrains. This is mainly due to their simpler, compact design and enhanced rotor control. We observe that the DFIM has proven to be a cost-effective, efficient, and reliable solution [1]. Even though the squirrel cage induction machine (IM) and the DFIM are very similar, an in-depth understanding of the DFIM requires a separate study and can be further used to explore its applications. In a comparison between synchronous generators and double-fed induction generators (DFIGs) that are used in wind energy systems, it was found that the DFIGs give a substantially better performance as they only use partial converter that uses 30% of the rated output of the generator as compared to the full-scale converter used in the synchronous generators that needs to be 100% of the rated output power of the generator [8]. The theory is that the DFIM rotor will essentially need less power to achieve the necessary performance, which can be employed as an added benefit in the automotive context where the DFIM is a secondary machine supporting the primary driving machine. This concept is particularly beneficial and is thoroughly researched in this study.

In the DFIM, we see that the stator and rotor are fed individually with power coming from the same source (grid, battery) through inverters. The typical supply configuration of the DFIM is when the stator is supplied by three-phase voltages directly from the grid at constant amplitude and frequency, creating the stator magnetic field. The rotor is also supplied by three-phase voltages that take a different amplitude and frequency at a steady state to reach different operating conditions of the machine (speed, torque, etc.) [2]. This is usually achieved by using a back-to-back three-phase converter, as represented in the simple schematic of the DFIG in Fig. 1.1. An appropriate rotor control strategy makes the DFIM very beneficial in electric vehicle (EV) applications by compensating for the shortcomings of an induction machine which will further be discussed in detail in the thesis.

The DFIM has been proven to be potentially a promising machine to be used in EV applications due to its advantages such as improved efficiency and extended torque-speed characteristics [13][26]. In the present scenario, we can see that the induction machines (IM) are used for the front wheel drive (FWD) along with the permanent magnet synchronous machine (PMSM) on the rear axle of an all-wheel drive application (AWD). Hence, the objectives of the thesis to apply the uses of DFIM in an automotive context will also be discussed. It is very important at this stage to note that all the previous studies done with DFIM in the EV context assume the fact that the DFIM receives controlled power sources at both the stator and the rotor end, through independent converters at both the stator and rotor, albeit through the same battery source. Similar configuration to the Fig. 1.1, but with a battery instead of the grid.

As the DFIM in this thesis is studied as a secondary machine (FWD) in an AWD configuration,

with the PMSM as the primary driving machine, the PMSM controller and inverter which decide the power required by the PMSM, will be the same fed to the stator of the DFIM. The PMSM stator and the DFIM stator are connected in parallel. Thus, the novelty in this study is that the stator of the DFIM does not receive a controlled voltage source through an independent inverter at the stator end. So, all the controls for the DFIM machine is carried out through an independent rotor controller and small micro-converter which is rated for very low power levels (3-6kW). This would then ensure a reduction in components needed in a regular squirrel cage IM such as inverters that are huge due to high power ratings and this also reduces the complexity of the overall electric drive system. There will be an increase in the overall space in the vehicle for other components as the packaging area of the drive system is reduced.

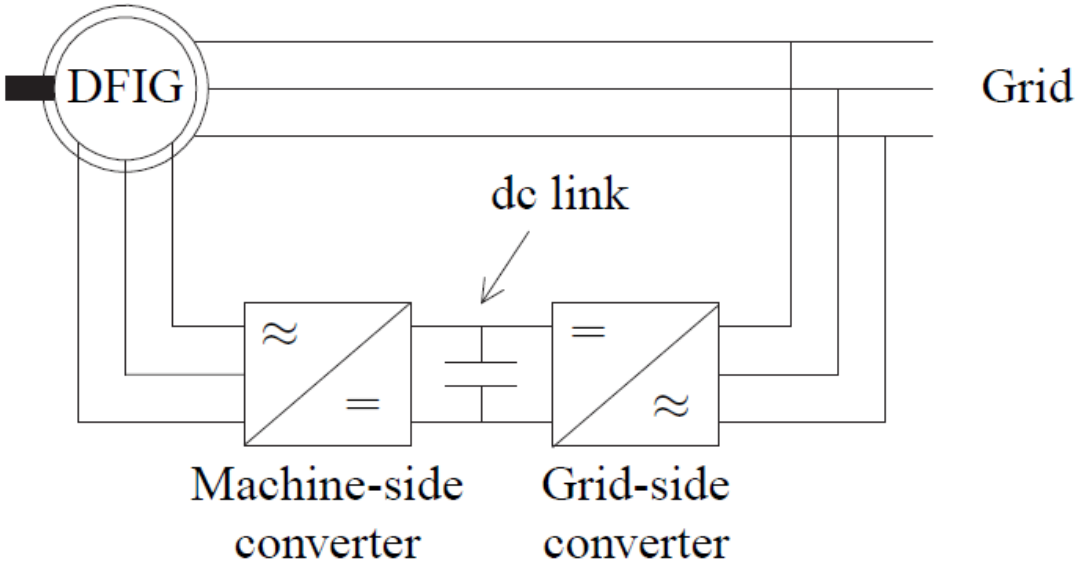

Figure 1.1: General DFIG system according to Petersson [19]

1.1 Thesis overview

The thesis is explained and divided into chapters and subsections as follows:

Chapter 2 discusses AWD in detail with components involved in the AWD, the need for an AWD in the automotive context, the present scenario with AWD, the proposed scenario in this thesis, the scope of improvement that the new proposed electric drive system provide, use cases of the DFIM in the proposed scenario, the anticipated benefits of having the DFIM for AWD, reduction in complexity of the overall electric drive system, issues to be tackled with DFIM in an AWD scenario.

Chapter 3 exclusively discusses all the details of the double-fed Induction Machine. The chapter discusses the working of the machine and its operating modes. The machine design parameters used this thesis are mentioned.

In chapter 4 we will discuss the modelling and control requirements, as well as the control strategy equipped in this thesis. The working of a DFIM will be tested as a standalone operation for a simple machine model setup and then expanded to see its application in the complete AWD setup along with the PMSM.

Chapter 5 discusses the complete analysis done with the DFIM. Here the different operating conditions are tested and comments on the feasibility of the machine are given. The results are

shown in detail with the necessary assumptions and limitations mentioned in chapter 2.

Further, in chapter 6, the conclusion and the future scope of the thesis are discussed.

1.2 Thesis objectives

The following are the research objectives outlined:

- Developing an independent rotor control strategy for the novel DFIM application in an automotive context.
- DFIM standalone model development with rotor controller to replace IM. Analyse the performance of the standalone DFIM with variable stator voltage source.
- Minimal rotor power usage to achieve the best performance from the DFIM.
- Develop a proper slip angle calculation algorithm to realize the standalone model of DFIM.
- Develop proper flux estimation and flux alignment algorithm for the DFIM rotor.
- Assessment of PMSM + DFIM combination against existing all-wheel-drive configurations.
- Observe the impact of including a PMSM with the DFIM standalone model.
- Reduce complexity of the overall electric drive system model.

1.3 Background

DFIMs (Doubly Fed Induction Machines) have been traditionally deployed in wind turbine applications. Hence, there is extensive research [12, 19] and documentation [1, 2] about using a Doubly Fed Induction Machine (DFIM) in generator mode. This is because these machines are well-suited for variable speed operation, a crucial requirement for maximising energy capture in wind power generation.

For automotive applications, DFIMs are increasingly favoured for high-performance electric drives, such as those used in traction systems for electric vehicles and vessels [18]. The inherent advantages of DFIMs, including their robustness, controllability, and ability to handle transient loads, make them well-suited for demanding traction applications where reliability and efficiency are critical.

In 1989, the Doubly-Fed Induction Machine was initially investigated as a variable speed motor that operated at double synchronous speed and was fed power on both sides without the need of a frequency converter [24]. After that, a number of authors worked with the same setup to conduct simulation and experimental investigations on variable speed control. By using an alternator that is attached to the rotor rings and powered at a variable speed, this control modifies the frequency of the rotor supply [24]. The development of power electronics in recent years has allowed for novel DFIM operating modes. The study of DFIM in generator mode applied to energy conversion systems has been the focus of many research projects.

In novel alternative approaches to use DFIM, studies suggest using the machine in motor mode for high power applications such as rail traction, marine propulsion, and metallurgy. In recent years, DFIM-equipped Variable Speed Traction Systems (VSTS) have been used in Electric Vehicle (EV) applications. An important part of the VSTS design process is choosing the traction motor for the EV system. Wide-ranging torque-speed characteristics, an increased power-weight

ratio, high drive system efficiency, high robustness, and reliability are the necessary attributes for an electric machine in the VSTS [28][26][25]. There are other studies like a new flywheel energy storage system based on a DFIM and a battery for use with micro-grids which can improve the power quality features, including the frequency and voltage [17]. Since choosing an appropriate initial rotor position is crucial when utilising the DFIM in direct starting strategy, there have been other studies highlighting the direct starting strategy of DFIM that present a thorough discussion on the effects of the initial rotor position on the DFIM starting performance. The application of the proposed method is simple without additional switches and switch-over algorithms [18].

Furthermore, advancements in power electronics and the adoption of newer and more control strategies, have further improved the chances of incorporating DFIMs by enabling more precise and efficient operation. Sophisticated control strategies, such as vector control and model predictive control, allow for precise regulation of torque and speed, resulting in improved overall system performance and energy efficiency. Several control strategies were developed with a focus on EV/HEV applications such as the dual current loop algorithm [13], dual electric port control [9], dual DTC (Direct Torque Control) [6] and vector control of DFIM [4]. There were also attempts made to study optimal control strategies with specific goals such as optimal torque control [27], MTPA strategy [11] and sensor-less operation [20].

The adoption of Doubly Fed Induction Machines for electric drives is a convergence of technological innovation and sustainability goals, driving forward the transition towards more efficient, flexible, and reliable electrical systems across various sectors. As research and development continue to push the boundaries of DFIM technology, their role in shaping the future of electric drives is guaranteed to expand even further.

1.4 Motivation of Volvo Cars for thesis

The thesis is intended to study the benefits and to find potential roadblocks (if any) of integrating DFIM with the company's (Volvo Cars') in-house developed battery technology. A successful integration of both these could potentially result in enhanced performance, efficiency, and reliability. In addition, this could potentially reduce the component costs (smaller converters) while allowing considerable weight savings.

While the battery technology enables efficient energy storage and management of the battery cells by dynamically adjusting their charging and discharging rates based on real-time demand and operating conditions, DFIMs can improve the efficiency and T-ω operating range. DFIMs also offer dynamic control under variable loading conditions. Introducing a DFIM in the electric drive system can reduce the number of components required by the front axle machine. This is because the inverter used for the stator control of the present Induction machine in the front axle can be replaced with a micro-controller to control the rotor independently. This all-wheel-drive configuration achieves similar performance to the machine controlled by the stator, but with much less power required by the rotor, resulting in a cost-effective solution. Thus, an integrated solution consisting of new battery technology and DFIM is seen as the best green solution for future personal mobility.

1.5 Limitations

- The thesis examines the viability of employing a DFIM as an assisting machine in an AWD configuration in an automotive context. The work only includes research using the PLECS software tool for 1D modelling and simulation. While approximate machine parameter estimates are provided, no real DFIM machine design is carried out in this thesis. Therefore, this study does not entail any actual machinery or experimental activity.
- This study uses the slip ring Induction Machine model that is available in the PLECS software

package. The thesis considers Slip Ring Induction Machine (SRIM) and adopts this design approach as the standard, even if other DFIM configuration methods can be applied to get equivalent results.

- As this machine is not explored much in automotive context, there is limited earlier reference work for DFIM in-vehicle applications with parallely connected machines.

- Does not include designing the DFIM. This means that the machine parameters are taken from a reference machine and also the effect of brushes/slip ring is negated. Although there are few solutions already discussed in previous work on brushless DFIMs such as cascading another wound rotor induction machine (WRIM) [10], a rotary transformer (inductive) [22], a plate capacitor (capacitive) [14], or even rotating power electronics [23], etc.

- The control method employed assumes perfect field orientation due to accurate sensing of the slip angle between the rotor flux and stator flux, which may not be the case in reality. There might be difficulties in getting the right slip angle calculation due to issues in sensors. (proper method to calculate the angle difference between stator flux and rotor flux.)

1.6 Hypothesis

- The Double fed Induction Machine working as a standalone machine will be tested first. This will determine whether the DFIM can be used as a primary single machine in automotive applications.

- It will be crucial to look into whether the performance of the DFIM independent rotor control strategy is comparable to that of a traditional IM, where the control is based on the stator control.

- Developing an optimal control strategy for DFIM to check the feasibility of the machine and determine the use cases where it will be beneficial.

- Identifying the important components to be included in the overall DFIM electric drive system in an automotive context.

- Determining the torque handling ability of the DFIM in AWD situation for smooth operation. Ease of operation of the machine in the AWD configuration.

1.7 Methodology

The thesis is planned to be executed according to a V-model of development where all the activities can be categorised into 4 different groups namely: design & implementation, testing, verification and validation. The left wing of the V-model focuses on understanding and identifying the metrics for the development and execution of the validation tasks in the right wing of the V-model as in a typical research problem.

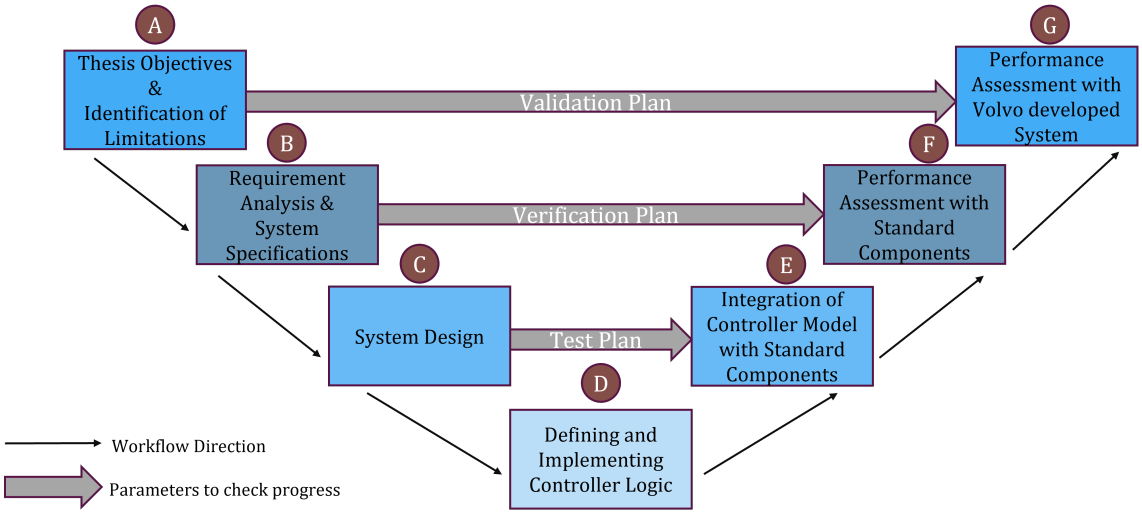

Figure 1.2: Thesis execution strategy with expected workflow

The execution of the thesis is planned in seven different phases namely:

- Phase A (Literature Review and Problem Definition)
- Phase B (Brainstorming)
- Phase C (Modelling All Wheel Drive with Doubly Fed Induction Machine)
- Phase D (Defining and Implementing Controller Logic)
- Phase E (Integration with Standard Components)
- Phases F and G (Feasibility and durability analysis of the integrated model at the component level and vehicle level

This section outlines the systematic approach adopted for the research on Double Fed Induction Machines (DFIM) for our Master's thesis. The methodology is divided into different phases, each detailing the specific tasks undertaken, tools utilized, and the rationale behind the chosen approaches.

Phase 1: Literature Review and Preliminary Model Exploration

Literature Review:

- Conducted an extensive review of existing literature on DFIM models.
- Investigated various control strategies employed for DFIMs.
- Studied different architectures of DFIMs and their implications on performance.

Familiarisation with PLECS and Initial Model Exploration:

- Simultaneously engaged with the PLECS software to understand its capabilities.

- Analysed the existing Double Fed Induction Generator (DFIG) Wind Turbine model to comprehend its working principles.
- Attempted to re-purpose the DFIG model to function as a motor for standalone testing.
- Identified a key limitation: the model relied on a stable grid source for the stator, while our thesis required a variable voltage source.

Phase 2: Custom Model Development

Brainstorming and Planning:

- Conducted multiple brainstorming sessions to devise the optimal method for independent rotor control in DFIM.
- Decided to build a custom DFIM model from scratch.

Initial Model Development:

- Developed a basic model without control mechanisms to observe the DFIM behavior under constant input conditions.
- Tested the machine in an All-Wheel Drive (AWD) scenario with a Permanent Magnet Synchronous Motor (PMSM) in parallel.
- Determined that using current sources directly was the most effective way to study the machine's behavior.
- Validated the machine's performance in terms of speed and torque but noted high power consumption at the rotor.

Phase 3: Control Implementation

Field Oriented Control (FOC):

- Initiated the implementation of Field Oriented Control to manage the high power consumption issue.
- Conducted initial tests with the PMSM in parallel at the stator and constant current sources at the rotor.
- Refined the control logic to include appropriate transformation angles and control strategies.
- Ensured the machine was controlled effectively with a constant voltage source at the stator.

Phase 4: Variable Stator Voltage Source Investigation

Variable Voltage Source Integration:

- Transitioned to using a variable voltage source for the stator to align with the thesis requirements.

- Conducted thorough testing to analyze the machine's performance under these new conditions.

Parameter Finalisation:

- Engaged in additional literature review to identify suitable DFIM parameters for our specific case study.
- Selected the optimal parameters to ensure accurate and reliable results for our research.

Model Implementation Adjustments:

- Modified the machine model to provide an open-loop torque reference for calculating current references.
- Utilized a speed controller to simulate PMSM machine speed, with the torque output serving as the load torque to the DFIM.

Phase 5: Control Strategies

Current Controller Implementation:

- Implemented a current controller in the FOC to provide voltages to the rotor side of the DFIM.
- Tested the rotor with voltage sources, but due to unresolved issues, the models with voltage sources at the DFIM rotor were not finalized.
- Assumed a transfer function of 1 for the ideal current controller at the DFIM rotor to simplify the analysis.

This comprehensive methodology enabled us to systematically address the challenges encountered during the research on DFIM. By progressing through clearly defined phases from literature review and initial explorations to model development and control logic implementations, we were able to build a robust model and achieve our research objectives effectively. Despite some challenges in finalising models with voltage sources at the DFIM rotor, the adaptations made allowed for meaningful insights and practical applications in our study.

1.8 Verification methods

In this process, the plan is to compare the existing configuration against the desired configuration that includes the DFIM on the following bases:

- The DFIM working validated at steady state condition with constant operating points of speed and torque.
- Vehicle level performance for different drive cycles such as WLTC, repeated acceleration profiles and Volvo in-house drive cycles

- Vehicle level performance under different test scenarios such as overtaking manoeuvres, uphill driving
- Component level performance for different operational characteristics such as T-ω characteristics, regeneration capabilities, transient behaviour
- Efficiency of the overall vehicle performance after deployment of the DFIM controller
- Overall power consumption by the DFIM machine to provide the extra torque required in AWD scenario. Also, the power consumption when the DFIM machine is not in use as the primary machine (PMSM) is driving the vehicle.

2

Electric drives

This chapter focuses on electric vehicles (EVs) with all-wheel-drive (AWD) systems. It will explain the current state of AWD technology in the automotive industry and the proposed new scenario. The DFIM will be discussed in detail, including how it is used in the proposed AWD system and its operating conditions. The chapter will also describe the layout of the AWD system using DFIM and the expected benefits. Additionally, it will outline the issues that need to be addressed and the goals of the proposed system. The issues to be tackled in such an AWD system with DFIM will be addressed in this chapter.

As discussed in chapter 1, the present combination for an AWD in an electric vehicle at Volvo Car Corporation is (IM - front axle + PMSM - rear axle), but this thesis focuses on a new configuration with (DFIM - front axle + PMSM - rear axle). An induction machine in an all-wheel-drive case makes sense for a number of reasons, including the absence of rare earth materials, the ability to extract maximum power from the system over a wide speed range, durability and reduced wear, high efficiency in low-power regions, reduced manufacturing costs, etc.

2.1 All wheel drive configuration

In the field of electric vehicles (EVs), the all-wheel drive (AWD) configuration is notable for its ability to enhance traction, stability, and overall performance. EVs have the flexibility to use multiple electric motors, which can significantly improve the effectiveness of AWD systems. AWD systems in EVs distribute power to all four wheels and have precise control over the torque distribution to each wheel, improving vehicle handling, especially in conditions like rain, snow, or off-road environments. It is seen that the torque distribution capability in the all-wheel-drive is very useful in difficult terrains and splitting the torque between the front and rear axle is discussed in a study conducted on AWD [3].

AWD systems can be of various types such as:

- Single machine setup: The machine that is connected to a drive-train that splits power between the front and rear wheels. While effective, it involves complex mechanical components, increasing the system's weight and reducing overall efficiency.
- Two machine setup: In this setup, the front and rear axles are powered by separate machines. Without requiring a lot of mechanical links, this setup gives more control over each of the axles and traction while achieving an appropriate balance between performance and complexity.

- Four machine setup: Each wheel is powered by an individual machine, allowing for the highest level of control and precision. This setup enables advanced torque vectoring, where power distribution to each wheel is finely tuned for optimal performance and handling, but adds on extra cost.

In the present setup, the AWD system featuring the IM & PMSM combination incorporates individual controllers on the stators of both machines. This configuration provides improved control over current distribution when both machines are engaged. The power distribution becomes more straightforward, enabling the establishment of an optimal and efficient operational setup for the machines. This approach ensures that even the induction machine, typically considered the secondary unit, can operate at its peak efficiency.

The electric drive train for the all-wheel-drive (AWD) system in this thesis integrates the electric machines DFIM & PMSM. This approach introduces a novel methodology, as the DFIM is managed by a micro-converter (Inverter + Rotor controller) designed for lower power ratings compared to conventional inverters used for standard induction machines or PMSMs. In this configuration, the power source is paralleled with both the DFIM and PMSM. The control of the PMSM machine dictates the voltage input to both the PMSM and the stator of the DFIM. Notably, independent control of the power supplied to the DFIM stator is absent; instead, precise control of the DFIM rotor is employed to ensure optimal performance through field-oriented control. Effectively, removing the inverter at the stator from the front machine reduces the components used in this drive train.

Scenarios in which the DFIM will be useful:

- Full power requirement from the front wheel (front wheel drive).
- Instantaneous extra torque requirement at the front wheel.
- Power split between front and rear machines.

A major advantage of the DFIM is that the power flowing to the rotor is a fraction of the power flowing through the stator. The power electronic equipment only has to handle a fraction (20–30%) of the total system power [19]. If we neglect the losses, the percentage of power is equal to the percentage of speed variation around the synchronous speed [5].

2.1.1 Induction machine all-wheel-drive

The present all-wheel-drive (AWD) features an Induction machine (IM) at the front axle. The IM has its own independent inverter at the stator that provides controlled supply of voltages. The IM relies on its rotor slip relative to the synchronous speed to generate the induced rotor current, this in turn helps in generating the torque from the machine. In an induction machine AWD setup there is usually a torque split ratio between the front and rear axle machines. The permanent magnet synchronous machine (PMSM) is usually the rear machine (primary machine). The PMSM machine is much more efficient than the induction machine as it exhibits high torque density, wide speed-torque range and compact size due to the strong magnetic field that is constantly provided at the rotor by the rear earth materials. The induction machine on the other hand has to completely rely on the external power source to provide the torque, although the advantage in the induced currents in the IM is that the machine is self-starting.

There are several studies based on Induction machines with permanent magnet synchronous machine combination for all-wheel-drive applications, where they have discussed that this dual-motor system offers a balanced and adaptable solution for contemporary EVs by utilizing the great performance and efficiency of PMSMs along with the robust and affordable nature of IMs. The

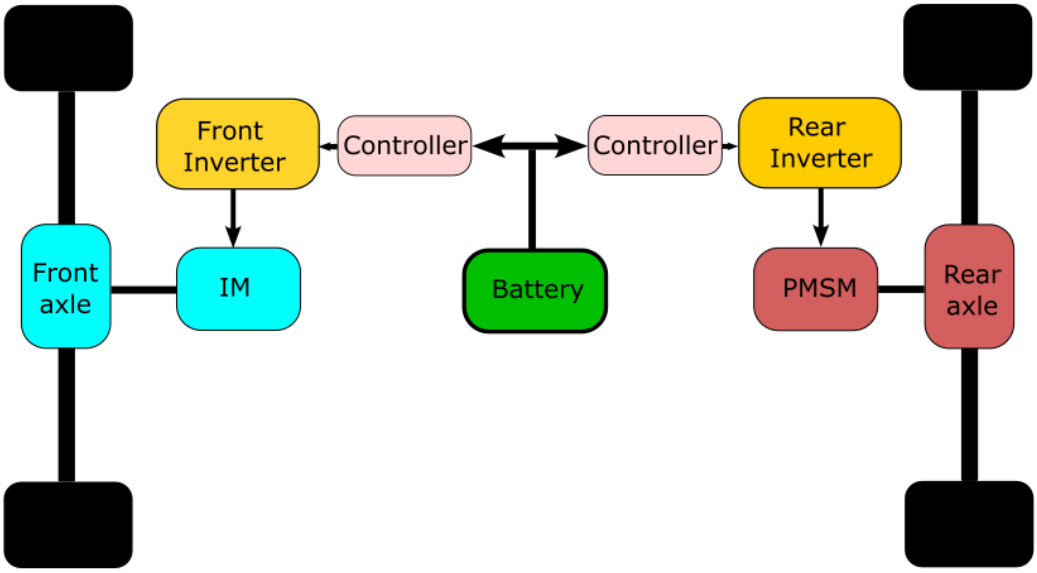

Figure 2.1: Induction machine all-wheel-drive layout representation

vehicle's capacity to manage different road conditions is further optimized by advanced modelling and control strategies, which make this a useful and efficient method of improving EV performance. The ability to tune the performance as needed and precise control of the traction forces makes it suitable for both high-efficiency driving and high-performance applications [16].

As the IM works with an inverter that has to be rated for a higher power supply at the stator end, the space utilized by the inverter in the IM AWD configuration is much more as compared to the DFIM configuration studied in this thesis. Here the IM and the PMSM have their own inverters, controllers, and other power electronics involved in the whole drive system. The battery supplies power through the inverters to each of the machines at the front and rear axles independently and in a controlled manner. This is the major difference between the present IM AWD system and the DFIM AWD that will be explained thoroughly in this thesis.

2.1.2 Double fed Induction Machine all-wheel-drive

The DFIM (Slip-ring induction machine is considered for modelling purposes) is beneficial in this AWD setup as this gives additional degrees of freedom of control at the rotor side. The stator circuit of the DFIM is connected to the PMSM stator, while the rotor circuit is connected to a small converter through slip rings. By controlling the rotor currents, it is possible to control the extra torque requirements to be met by the front machine in situations where it is needed and this helps the machine operate at a wide speed range. Although the DFIM is most often used as a variable-speed, constant frequency generator such as in wind power, lately the DFIM is proposed as a potential candidate for EV/HEV applications. This is due to its extended regions of both constant torque and constant power operation. [13]

As it is already established in 1, this thesis will investigate a dual-motor configuration for all-wheel-drive. The DFIM will be setup for the front wheel drive and the PMSM for the rear wheel drive. The PMSM will be used as the primary machine in most of the driving conditions, although in cases of additional torque requirements from the front wheels, the DFIM will be engaged to provide for the extra torque (ΔT).

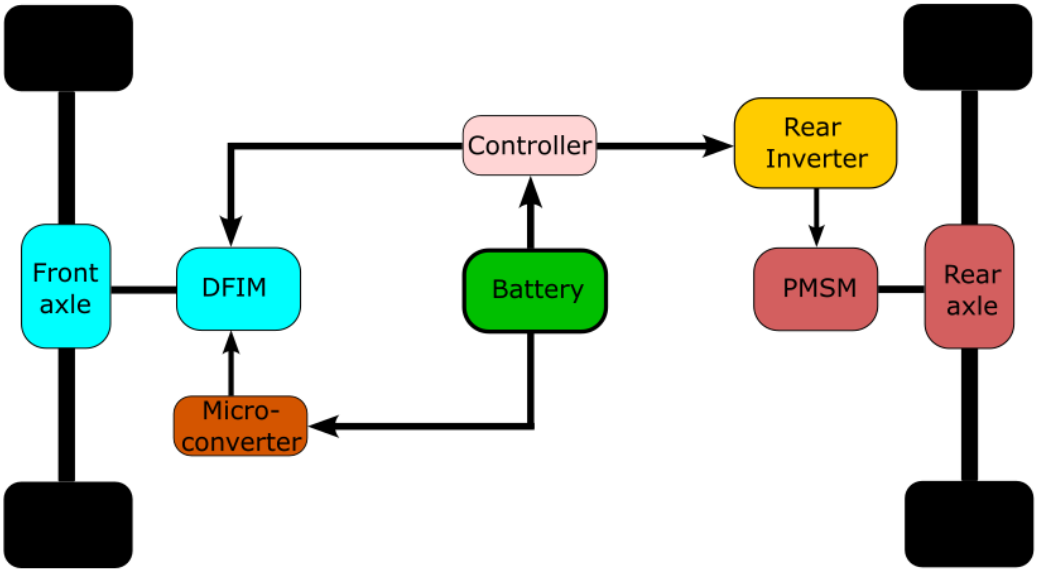

Figure 2.2: DFIM all-wheel-drive layout representation

The battery source is connected in parallel with both DFIM and PMSM machines in our case study, where the PMSM and the DFIM stators receive the same voltage supply depending on the requirements of the PMSM machine. The machine requirements are provided by the PMSM controller, which depends on the PMSM machine configuration. Hence, the power supply to the DFIM stator is not in accordance to the DFIM machine configuration. In this situation, the smaller independent rotor controller for the DFIM will be the main focus of this study to achieve similar performance from both the machines in case of an all-wheel-drive.

2.2 Complete AWD model components

The electric drive system consists of a battery pack, power converter, electric machine controller, electric machine, transmission, and wheels. In this study, the focus will be on the Double-fed Induction Machine and the novel rotor controller for controlling the machine.

In Fig. 2.3, the setup for a dual motor configuration is shown, which will be the basic setup at which the DFIM is set to operate. Fig. 2.4 shows the dual motor configuration, but with the inclusion of the current controller at the rotor side of the DFIM. The setup shown in Fig. 2.4 will be the actual setup in an AWD scenario, although, for this study, the current controller is considered to be ideal and for ease of the study on the feasibility of this AWD setup, the current sources are used on the rotor windings of the DFIM.

2.2.1 Mechanical machine model

The machine model includes the load acting on the DFIM. The reference torque for calculating the q-current (Iq*) comes from the speed controller. The mechanical model of the vehicle is based on the equation 2.2.1.

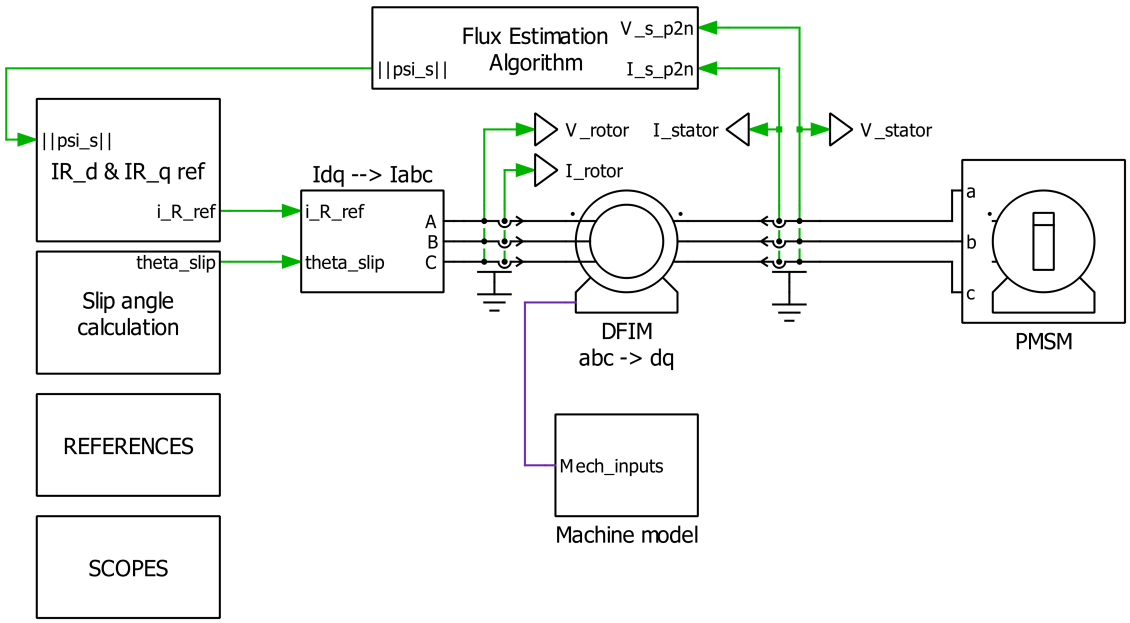

Figure 2.3: Double-fed Induction Machine with Permanent magnet synchronous machine all-wheel-drive configuration PLECS model (with current sources at the DFIM rotor)

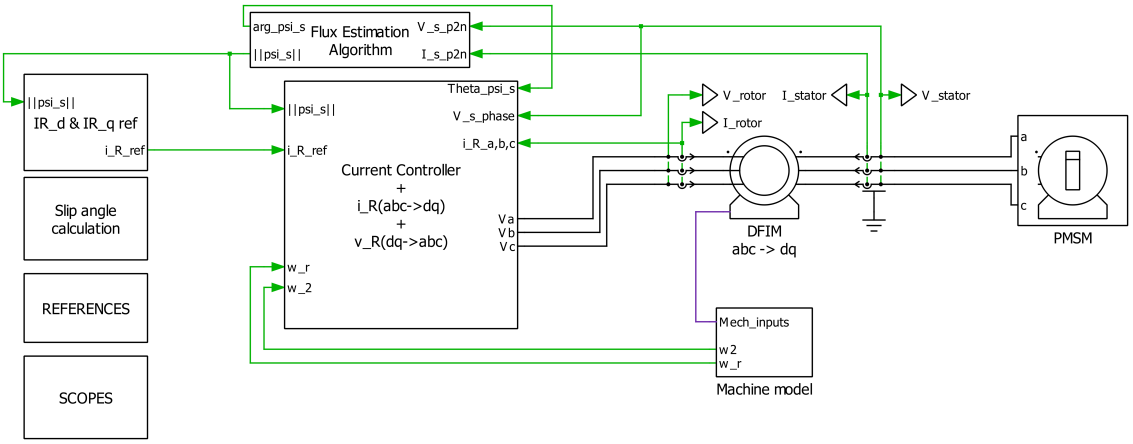

Figure 2.4: Double-fed Induction Machine with Permanent magnet synchronous machine all-wheel-drive configuration PLECS model (with voltage sources at the DFIM rotor)

$$\frac{J}{n_p}\frac{dw}{dt} = T_e - T_L \tag{2.2.1}$$

Inertia (J) is defined for the machine, ($\frac{dw}{dt}$) is the change in speed of the machine, Electrical torque (T_e) is the electrical machine output torque, mechanical load torque (T_L) applied to the machine and n_p is number of pole pairs.

2.2.2 DFIM stator power source

In this thesis, the DFIM machine is in parallel with the PMSM, and the investigation is based on a situation where there is no control over the power/voltage source connected to the DFIM stator. The controlled voltage source being fed to the PMSM is the same that is given to the DFIM stator as well. The DFIM rotor controller is responsible for the performance of the DFIM in situation of

extra torque requested at the front wheels. The DFIM stator is always connected to a constant AC source coming from the battery which is connected in parallel to PMSM.

2.2.3 DFIM rotor power source

The DFIM rotor is connected by a three-phase AC supply. This can be done in two possible ways:

- Placing a back-to-back converter with a DC link capacitor in between the stator AC source and the rotor.
- Giving an AC source through a DC link capacitor and a converter.

At the rotor side, the position controller gives the reference speed required by the speed controller to give the torque reference for the calculation of the rotor current references(i^*_{Rd}&i^*_{Rq}). The speed controller is a proportional-integral (PI) controller. This contains the active damping and the anti-windup factors taken into consideration for the machine in consideration. The inner current controller uses the current references being calculated to get the appropriate rotor voltages to be fed to the DFIM rotor.

2.2.4 Power electronics

Power electronic devices are used in an electrical system to vary the power requirement and control electrical circuits. The different types of power electronics used in this thesis are listed below.

Active components: These components control the flow of electrical energy actively and adjust the voltage and current requirements. The components depend on factors such as switching frequency, load current, and voltage.

- MOSFETs - These are used due to their high switching speeds, compact size, and lower power consumption.
- IGBTs - These are used due to their high voltage/current handling and lower saturation voltage.

Passive components: These components do not require an external power source to operate. They cannot control the flow of electrical energy, instead, they have predictable properties that can be used for applications such as energy storage and filtering.

- Inductors - Inductors are current stiff components used in the model to filter out the current transients and sudden surges to smooth the overall current flow.
- Resistors - Restrict the flow of electric current in the circuit and ensure current is flowing at appropriate levels.
- DC Link capacitors - Capacitors are voltage stiff components. These are used to store the excess currents, and reduce the voltage ripples in the circuit. Mainly used in converters to provide stability to the DC bus voltage.

2.3 Double fed Induction Machine operating scenarios

In an all-wheel-drive system, the front machine is often a secondary machine that helps the rear primary machine (PMSM in this study) when more torque is needed at the front wheels. Typically, these secondary machines are small and robust and are configured to operate with split torque outputs on the wheels, sharing the rest from the primary machine. In the table 2.1 the instances where the DFIM is anticipated to be operating in an AWD system during the course of this study are shown.

Operation	DFIM	PMSM	Mode
Motor Mode	ON	ON	AWD
	OFF	ON	RWD
	ON	OFF	FWD
Generator Mode	ON	ON	AWD
	OFF	ON	RWD
	ON	OFF	FWD
Power distribution	40	60	AWD
	0	100	RWD
	100	0	FWD

Table 2.1: DFIM operation in AWD scenarios

The operating conditions of machines in vehicles give the following modes:

1. AWD: All-wheel-drive
2. RWD: Rear-wheel-drive
3. FWD: Front-wheel-drive

2.4 Issues to be tackled with the DFIM system

- The DFIM is not the primary machine in the AWD setup. As it will be acting as an assistive machine, the thesis focuses majorly on tackling the situation by disengaging the DFIM by changing the rotor power, as the stator power source is always engaged with the parallelly connected battery source and the PMSM stator.
- As the stator of the DFIM is always engaged with the power source, there will be problems to deal with such as magnetization losses. There is no real control over the stator voltage and currents directly. These have to be controlled through the rotor power source. But, this rotor power has to be minimal, as the losses have to be reduced as much as possible.

2.5 Benefits of DFIM system

- As discussed earlier, the key motivation to pursue this thesis will be to see that minimal power is supplied to the rotor to get the best performance from the DFIM system.
- The DFIM can be used constantly with an efficient split between the front and the rear machines, which might reduce the losses during the disengaged scenario of the DFIM.

2.6 Assumptions

To choose a new electric drive system configuration, this study makes some assumptions. The following aspects are essential to the drive system and are considered to be as follows:

1. All the power electronics involved in the electric drive system are assumed to be ideal in this study.
2. The battery source equipped in an actual AWD system is not used here, instead a representative power source is used for convenience of the study.
3. Power is supplied to the rotor and stator of the DFIM in several methods, but the study assumes that the rotor is powered by current sources and the stator is powered by a stator voltage source. It is assumed that the current controller is ideal. This implies that the voltage source (V_{abc}) that comes out from the current controller would ideally provide the rotor with the same amount of power as the current sources on the rotor.
4. Given that the PMSM will be the primary driving machine and that it will determine the speed at which the DFIM must drive, the stator voltage block is proportionate to the speed demanded by the PMSM. As the speed increases, the stator voltage block utilizes linear voltage normalization and increases accordingly. The machine's base speed is considered to be around 6000 RPM at 800V.
5. The slip angle is supposed to be calculated by taking the difference between the stator and the rotor fluxes as given in 4.3.1. But in this study, for modelling purposes, the slip angle calculation (4.3.1.2) is done based on the difference between the angular frequency of the stator and the rotor, which is then integrated to get the θ_{slip}.

3

Double fed Induction Machine

The Double Fed Induction Machine (DFIM) has emerged as an important discovery in the field of electrical engineering, especially in applications that demand high efficiency, flexibility, and precise control, such as wind energy generation, variable-speed drives, and power systems. Unlike traditional induction machines, which typically rely on a single set of windings on the stator, the DFIM distinguishes itself by employing two independently controlled three-phase windings such that one is on the stator and the other on the rotor. This unique dual-feed configuration gives the DFIM the remarkable ability to operate efficiently over a wide range of speeds, including both sub-synchronous and super-synchronous operations, thereby offering substantial advantages in terms of energy efficiency and operational range.

The stator of the DFIM is composed of three windings, each displaced by 120° in space, which collectively form a rotating magnetic field when energized by a balanced three-phase AC voltage. This rotating magnetic field induces an electromotive force (EMF) in the rotor windings according to Faraday's law of electromagnetic induction:

$$\epsilon = (v \times B)L \tag{3.0.1}$$

Applying voltage directly to the rotor, using brushes and slip rings, generates a rotor current along with the current that is induced in the rotor windings as a result of the induced voltage in the windings. The interaction between this rotor current and the stator's rotating magnetic field produces the torque needed to drive the machine, as Laplace's law of electromagnetic force describes. This induced force in the rotor is crucial because it directly affects the machine's mechanical output

$$F = i.(L \times B) \tag{3.0.2}$$

where:
F = Electromagnetic force (N)
i = current in the rotor conductor (A)
ϵ = induced emf in single rotor conductor (V)
v = speed of the conductor w.r.t stator flux (m/s)
B = Magnetic flux density (T)
L = length of the conductor (m)

One of the defining characteristics of the DFIM is its use of brushes and slip rings to facilitate power transmission to the rotor windings. While these components enhance the machine's ability to control rotor current and thus improve its overall performance, they also introduce certain maintenance challenges. The mechanical wear and tear on the brushes and slip rings necessitate periodic maintenance, which can affect the machine's reliability and operational costs. However, significant advancements in recent research have led to the development of brushless DFIM configurations. These innovations aim to eliminate the need for brushes and slip rings, thereby reducing maintenance requirements and increasing the machine's reliability, while still retaining the key benefits of the DFIM's dual-feed design.

In the DFIM, the relationship between the stator supply frequency (f_s) and the rotor speed is governed by the machine's synchronous speed, defined by the equation 3.1.1, where n_p is the number of pole pairs in the machine.

Moreover, the versatility of the DFIM extends beyond energy generation to include its application in various industrial processes, where the precise control of speed and torque is crucial. The ability to operate in both motoring and generating modes, combined with the capacity to transfer power bidirectionally between the rotor and stator, further amplifies the DFIM's utility in modern electrical systems. This bidirectional power flow capability enables the DFIM to contribute to grid stability and power quality, particularly in scenarios involving fluctuating power demands or variable energy sources.

3.1 Electrical equations

The mechanical synchronous speed (rpm), n_s, equals:

$$n_{syn} = \frac{60 f_s}{n_p} \tag{3.1.1}$$

Angular frequency of the stator voltage (rad/s):

$$\omega_s = 2\pi f_s \tag{3.1.2}$$

The mechanical speed of the rotor (rpm):

$$n_r = \frac{30}{\pi}\Omega_r \tag{3.1.3}$$

The electrical speed of rotor (rad/s):

$$\omega_r = \Omega_r n_p \tag{3.1.4}$$

Turns ratio :

$$u = \frac{N_s}{N_r} \tag{3.1.5}$$

Slip, s :

$$s = \frac{\omega_s - \omega_r}{\omega_s} \tag{3.1.6}$$

$$\omega_s - \omega_r = \omega_{slip} \tag{3.1.7}$$

$$\theta_{slip} = \int \omega_{slip} \tag{3.1.8}$$

Depending on the sign of the slip, the machine can be distinguished to be working at three main operating modes:

1. Subsynchronous operation: $\omega_r < \omega_s \Rightarrow s > 0$

2. Hypersynchronous operation: $\omega_r > \omega_s \Rightarrow s < 0$

3. Synchronous operation: $\omega_r = \omega_s \Rightarrow s = 0$

3.2 Double fed Induction machine parameters

The book "Design of Rotating Electrical Machines" [21] outlines all the steps that must be followed while designing a new machine for the first time B.1. However, reference values were chosen as machine parameters rather than precisely following this process because the focus of the thesis was not on the designing the machine, but rather understanding the behaviour in AWD scenario and further taking the call on developing the complete machine design according to the procedure.

The DFIM taken into consideration in this study is anticipated to be a machine of about 215 kW, which will resemble induction machines presently in use in the industry. There were no explicit references to the machine itself, with the preset machine settings, because this is a new machine being evaluated in this all-wheel-drive application. This machine has never been tested in an AWD scenario like this one, and as of right now, no changes have been made to its design. Accordingly, based on a reference provided in a book on double fed induction modelling and control [1], it is assumed that the machine parameters are within a certain range of values.

The machine parameters shown for a 250kW machine in the book [1] is used as reference for the DFIM in this study as given in 3.1 and the performance of the same was checked and depending on that, some parameters are modified to suit the simulation. The resistances and inductances have been modified using the following equations 3.2.5, which are based on the reference book. The values were found to be well within possible range of an actual DFIM and this can further be validated by the performance and other parameters involved in the machine which will be discussed further.

$$u = \frac{N_s}{N_r} \cong \frac{6}{15} \tag{3.2.1}$$

$$R_r^{'} = \frac{R_r}{u^2} \tag{3.2.2}$$

$$L_{r\lambda}^{'} = \frac{L_{r\lambda}}{u^2} \tag{3.2.3}$$

$$L_{s\lambda} \cong L_{r\lambda}^{'} \tag{3.2.4}$$

$$L_m = \frac{4.2mH}{u^2} \tag{3.2.5}$$

Characteristic	Parameters	Value	Unit
Number of pole pairs	n_p	2	–
Turns ratio	u	0.4	–
Stator resistance	R_s	20	$m\Omega$
Rotor resistance w.r.t the stator	R_r	20	$m\Omega$
Rotor resistance	$R_r^{'}$	125	$m\Omega$
Rotor leakage inductance w.r.t the stator	$L_{r\lambda}$	0.2	mH
Rotor leakage inductance	$L_{r\lambda}^{'}$	1.2	mH
Stator leakage inductance	$L_{s\lambda}$	1.2	mH
Magnetising inductance	L_m	26.2	mH
Inertia	J	0.3	–
Stator flux	ψ_s	0.001	Wb

Table 3.1: Double fed Induction Machine parameters

4

Modelling and control requirements

The chapter is dedicated to introducing the modelling and control requirements specific to the DFIM to achieve AWD capabilities. On one hand, this chapter discusses the mathematical models (electrical equations and transfer functions) of the various components in the EV architecture such as the DFIM, mechanical load (driver model), a voltage source. On the other hand, this chapter also focuses on the control requirements such as the gamma model of IM, stator flux orientation vs grid flux orientation, reference frames, etc.

There are various methods discussed in the literature to control the DFIM but the control technique used on the rotor of the DFIM in this thesis is field-oriented control (FOC). To control the rotor currents of the DFIM, the reference frame of the direct component of the rotor current is aligned with the stator flux.

This chapter focuses on developing a broad framework of modelling and control requirements specific to the DFIM in the context of this thesis's objectives. This chapter serves as a theoretical basis to understand and analyze the system model in terms of its constituent equations that describe the mechanical, electrical, and flux dynamics of the system. In doing so, the key differences between a conventional induction machine and the DFIM in terms of complexity and controllability are elaborated.

It is to be noted that DFIM stator voltages are decided based on the controller for PMSM mounted on the rear axle as part of the EV architecture to achieve AWD capabilities. There will be no stator-mounted controller for the DFIM. Instead, a microcontroller on the rotor will handle all DFIM controls. The stator of the DFIM along with the stator of the PMSM is controlled by the PMSM controller. Hence, we get a variable frequency voltage input to the DFIM stator, unlike an induction machine with controlled stator voltage with an independent inverter and controller.

To begin with, the modelling conventions followed in this thesis are discussed. This includes the space vectors, and the phase-locked loop type estimator (PLL). Following this, the mathematical models are elaborated, which include the machine model of DFIM in T-equivalent form (for modelling) and the Γ-model form (for control). Finally, the layout of the complete model is discussed, providing an overview of the complete system.

There are various methods discussed in the literature to control the DFIM but the control technique used on the rotor of the DFIM in this thesis is field-oriented control (FOC). To control the rotor currents of the DFIM, the reference frame of the direct component of the rotor current is aligned with the stator flux. Most control algorithms for DFIMs are based on field-oriented control, similar to those used for squirrel-cage machines. When two converters are used, the problem is simpler because both the stator and rotor currents can be controlled. However, with only one

converter at the rotor and a variable stator voltage and frequency, the control becomes more complex than that of squirrel-cage machines. Despite this complexity, fluxes can still be estimated through measurements of the stator and rotor currents, with the flux magnitude determined by the stator voltages.

4.1 Modelling Conventions

4.1.1 Space vectors & coordinate frames of reference

The use of space vectors is to simplify the three-phase notation into a much simpler two-component vector form. Any electrical framework or equation can be represented as a space vector and depending on the frame of reference, chosen based on convenience can be transformed from one frame of reference to another. These frames of reference (Fig. 4.1 are defined based on the component of reference, for example, stator fixed frame ($\alpha - \beta$ reference frame) or any other reference frame that is aligned with a specific electrical quantity (d-q reference frame).

The transformation from three-phase notation to $\alpha - \beta$ notation and/or d-q notation can be done using the following equations and a specific choice of the constant K. For an RMS invariant transformation, $K = 1/\sqrt{2}$, and this is the transformation used throughout this thesis.

$$s^s = s_\alpha + j s_\beta = \frac{2K}{3}(s_a + a s_b + a^2 s_c) \tag{4.1.1}$$

$$s^s = s e^{j(\theta_s + \phi)} \tag{4.1.2}$$

$$s = s_d + j s_q = e^{-j(\theta_s)} s^s = s e^{j(\phi)} \tag{4.1.3}$$

Here, θ_s is the synchronous angle corresponding to the synchronous frequency ω_s, while ϕ is the phase shift angle which varies according to the desired frame of reference. The choice of ϕ is crucial in determining the reference frame and can significantly affect the accuracy of control logic, as can be seen in later sections of field orientation.

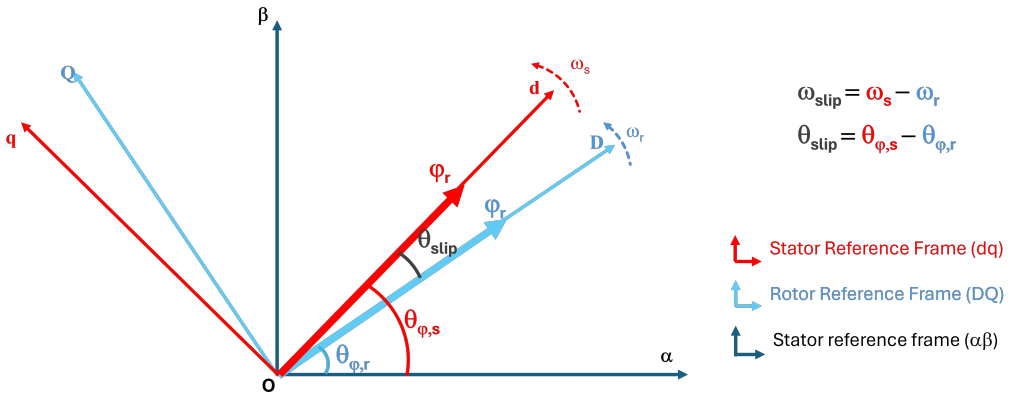

Figure 4.1: Coordinate frames of reference

4.1.2 Phase Locked Loop (PLL) type estimator

A phase-locked loop-type estimator is used for the estimation of the angle and frequency of a signal. It is used in the flux estimation algorithm to determine the stator flux magnitude and stator flux

angle. The PLL type estimator used in this thesis is discussed in greater detail in Petersson et al [19]. For this thesis, the PLL estimator used is a pre-defined block with a pre-defined controller logic modelled in PLECS.

4.1.3 Power in terms of space vectors

The instantaneous power P i.e., the active power consumption is calculated in a three-phase system by using the equation 4.1.4. Similarly, the reactive power Q is calculated as $Q = \frac{3}{2}\mathrm{Im}[v.i^*]$. This relation is utilized in imposing the reactive power control constraint, as explained in later sections.

$$P = v_a i_a + v_b i_b + v_c i_c = \frac{3}{2K^2}\mathrm{Re}[v^s(i^s)^*] = \frac{3}{2K^2}\mathrm{Re}[\mathrm{vi}^*] \tag{4.1.4}$$

For the amplitude invariant transformation, where $K = \frac{1}{\sqrt{2}}$:

$$P = 3\mathrm{Re}[\mathrm{vi}^*] \tag{4.1.5}$$

Similarly, the reactive power, Q, as the corresponding imaginary part of the equation 4.1.4 is shown below. This relation is utilized in imposing the reactive power control constraint, as explained in later sections.

$$Q = 3\mathrm{Im}[\mathrm{vi}^*] \tag{4.1.6}$$

4.2 Mathematical Models

This section covers the complete explanation of the modelling techniques used to accurately simulate the different components of the AWD system with DFIM, and the reasoning behind any assumptions made in order to arrive at these models. To provide a holistic understanding of the same, a top-down approach is followed to elaborate upon each of the components starting with an explanation of the system layout. This is followed by the explanation of the three major components of the system.

4.2.1 System Layout

The complete system layout (refer Fig. 4.2) consists of the electrical machines i.e., DFIM & PMSM (modeled along with its controller) and the micro-converter for DFIM rotor control. The system performance requirements are dictated by the driver model which are included as driving cycles.

The system layout is modeled in PLECS as a stand-alone DFIM model as shown in Fig. 4.3 where all the relevant subsystems are shown. As stated earlier, the DFIM stator is energized based on the PMSM controller logic which is shown in Fig. 4.2 as the 'Stator voltage' block. The '$Idq \rightarrow Iabc$' block and '$IR_d\&IR_qref$' are representative of the DFIM controller. The field orientation with stator flux is carried out using the 'Flux estimation algorithm' and 'slip angle calculation' blocks. The 'Machine model block' and the 'References' blocks together constitute the mechanical dynamics model and the driver model for the complete system.

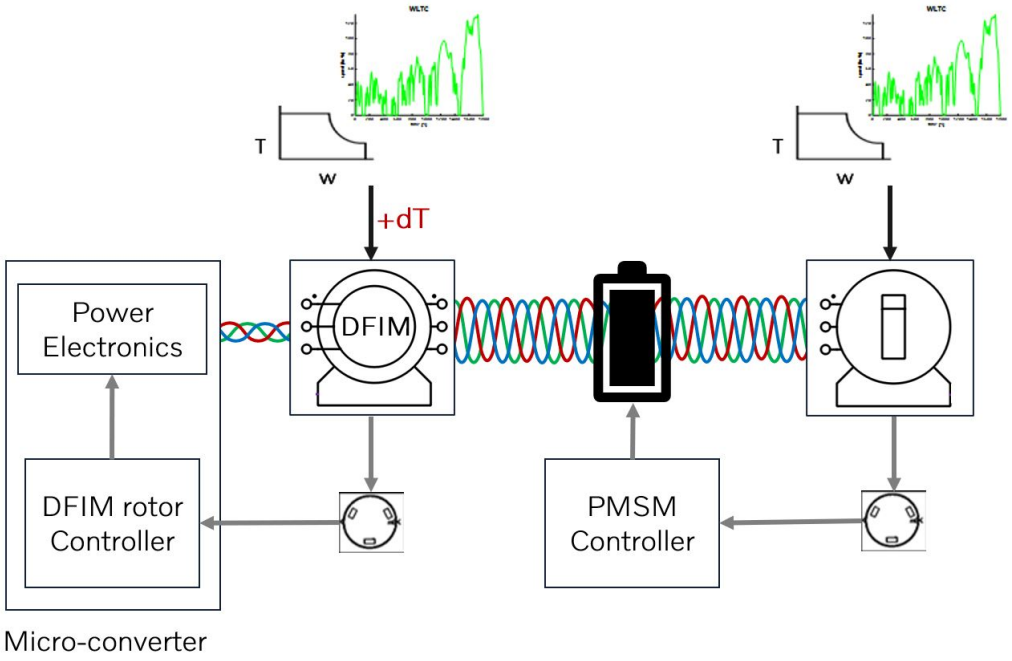

Figure 4.2: System layout for DFIM based AWD

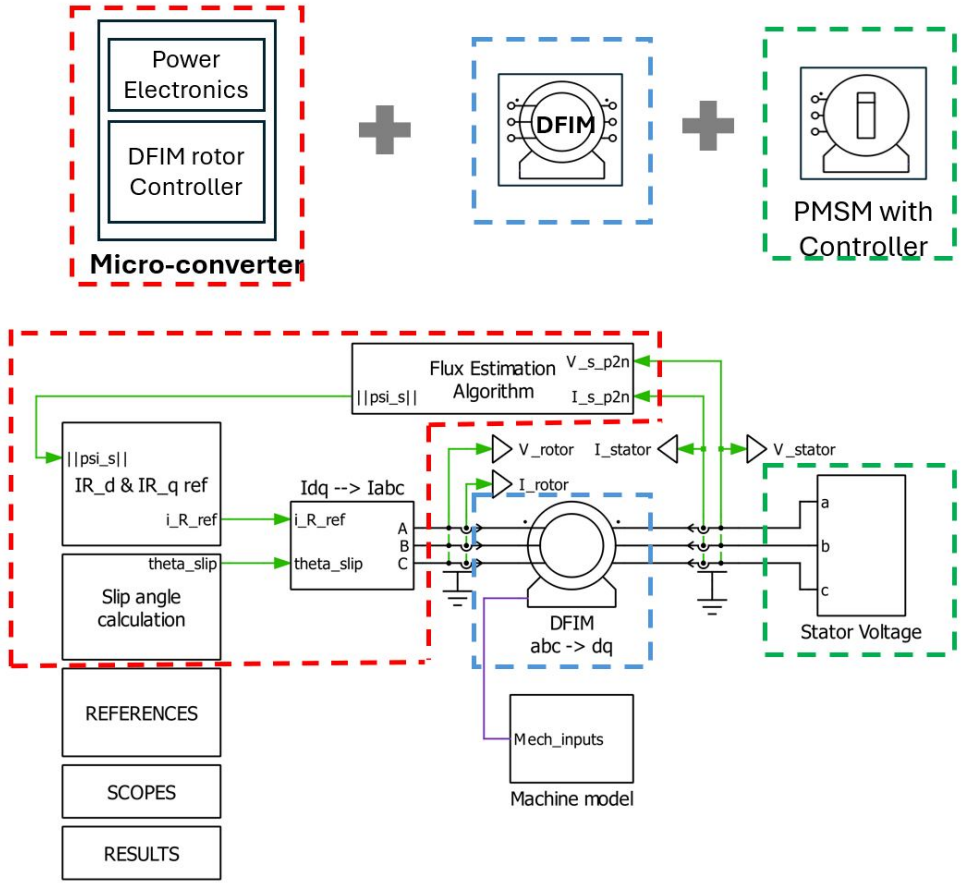

Figure 4.3: AWD system with DFIM model on PLECS

4.2.2 DFIM stator voltage model

The stator voltage block is represented in Fig. 4.4 below, which is modeled to be a variable voltage source at the stator of the DFIM depending on the speed reference. Here, the speed reference given from the driver profiles are considered to be the speed of the permanent magnet synchronous machine, which decides the speed of the vehicle in this study. Mechanical speed (rad/s) is converted to electrical speed in accordance with the reference speed provided in Sec. 4.3.3.3 while using it for conversion to voltages. The linear normalisation is done for calculating the voltage magnitude by using 6000RPM as the base speed for this DFIM. The voltage saturation is the limitation set by the power electronics that supply the voltage to the stator.

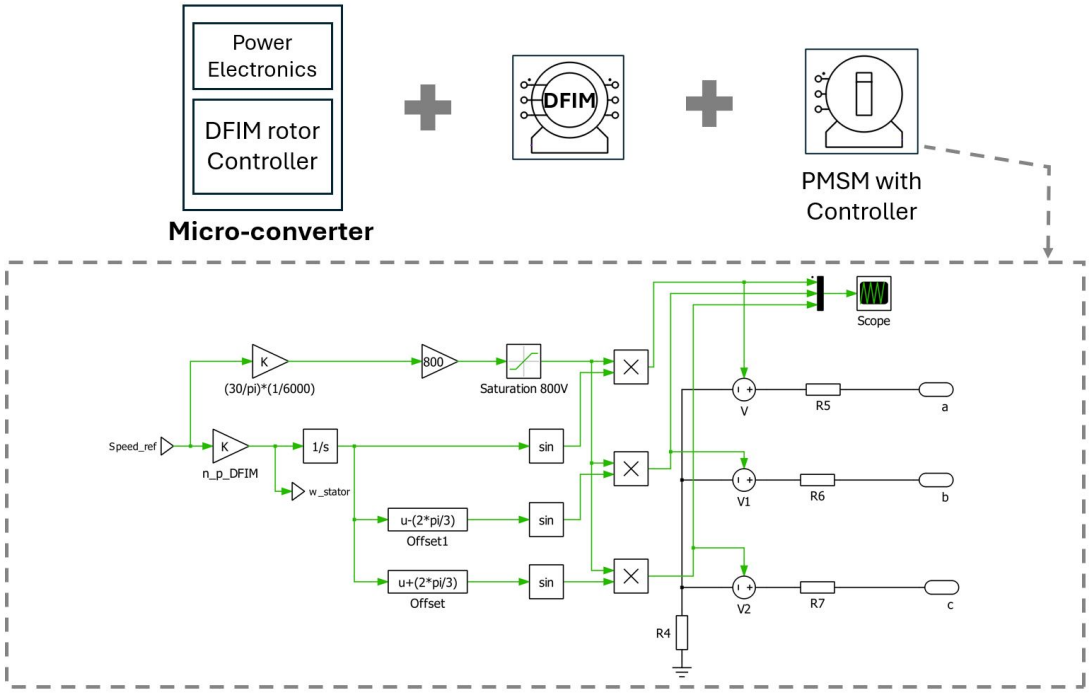

Figure 4.4: Simplified stator voltage model representative of speed variations on DFIM & PMSM stator

4.2.3 DFIM: Modelling

The modelling of DFIM requires two different approaches, one for simulation of the DFIM on PLECS (T-equivalent model) and the other for controller design (Γ-model). This can be observed in Fig. 4.5 & 4.6.

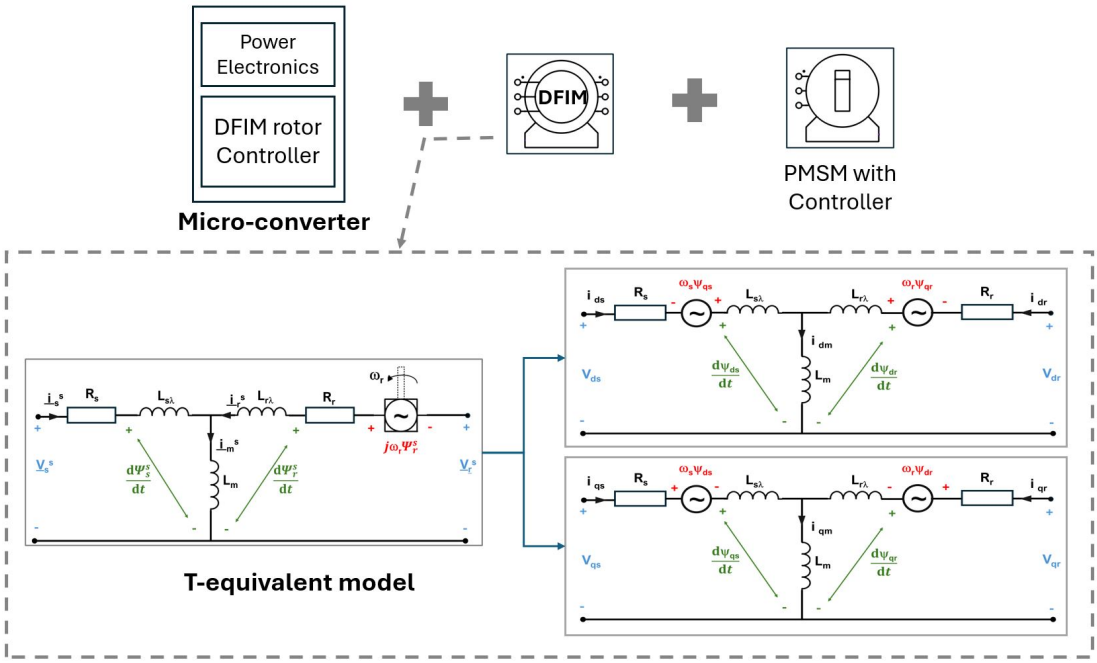

Figure 4.5: System layout with DFIM in T-equivalent model for simulation

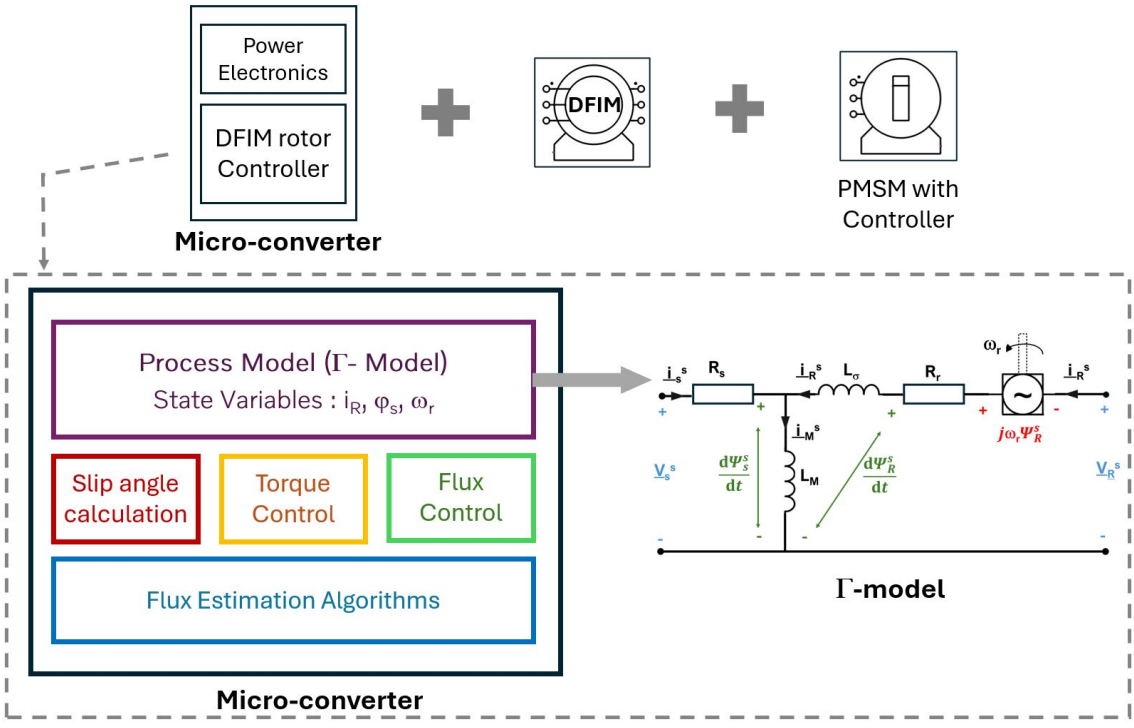

Figure 4.6: System layout with DFIM in Γ-model for control

With this understanding in mind, the following sections elaborate the above-mentioned mathematical models in greater detail along with necessary equations to describe the various electrical and mechanical parameters of interest.

4.2.3.1 DFIM: construction

The DFIM in its simplest form, can be represented as a stator and rotor with three windings each, as shown in the following Fig. 4.7. This is similar to a conventional induction machine, except for the fact that the rotor windings can also be excited in a DFIM.

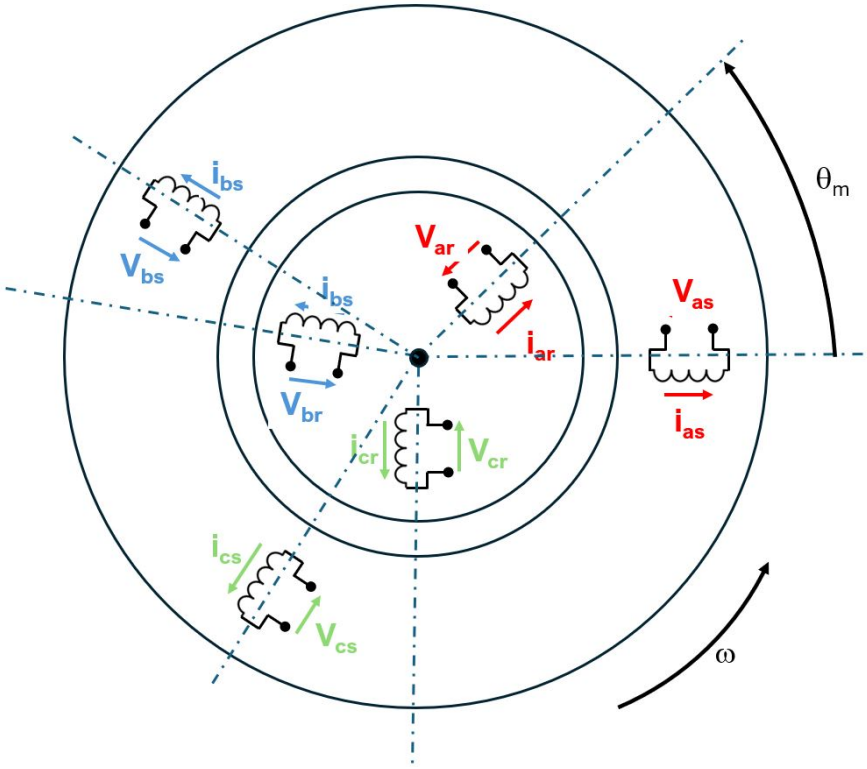

Figure 4.7: Simplified representation of a DFIM

The equivalent circuit diagram of the DFIM is as shown in the Fig. 4.8.

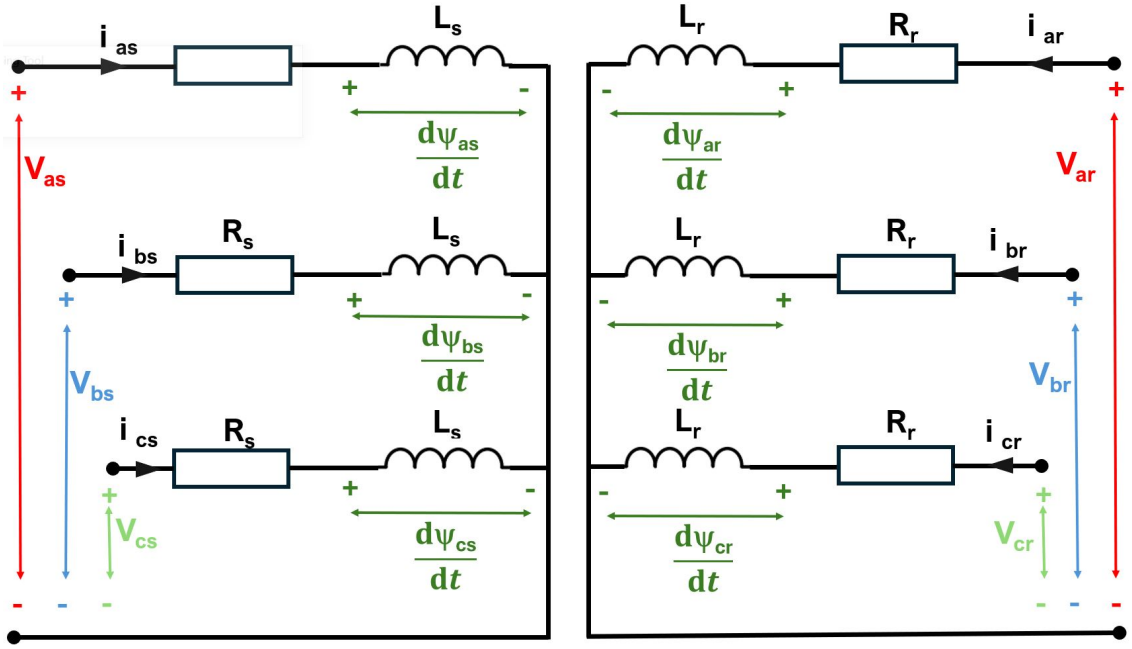

Figure 4.8: Ideal equivalent circuit of DFIM

For an ideal model, the three-phase voltage equations are as follows:

$$v_{as}(t) = R_s i_{as}(t) + \frac{d\Psi_{as}(t)}{dt} \tag{4.2.1}$$

$$v_{bs}(t) = R_s i_{bs} + \frac{d\Psi_{bs}(t)}{dt} \tag{4.2.2}$$

$$v_{cs}(t) = R_s i_{cs} + \frac{d\Psi_{cs}(t)}{dt} \tag{4.2.3}$$

4.2.3.2 DFIM: T-equivalent form

The T-equivalent form of the electrical circuit in a stationary reference frame after simplification (T-equivalent circuit) is shown in the Fig. 4.9.

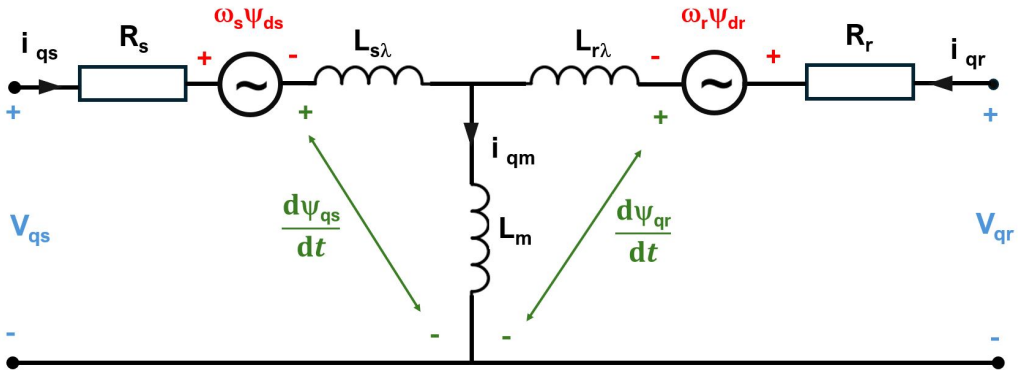

Figure 4.9: T-equivalent circuit of DFIM

This circuit as represented in the synchronous reference frame is as shown in the Fig .4.10. This equivalent circuit model is used for modelling purposes in the DFIM.

The voltage equations in the $d-q$ reference frame obtained through necessary space vector transformations are as follows:

Stator side:

$$V_s = R_s i_s + \frac{d\Psi_s}{dt} + j\omega_s \Psi_s \tag{4.2.4}$$

$$V_{ds} = R_s i_{ds} + \frac{d\Psi_{ds}}{dt} - \omega_s \Psi_{qs} \tag{4.2.5}$$

$$V_{qs} = R_s i_{qs} + \frac{d\Psi_{qs}}{dt} + \omega_s \Psi_{ds} \tag{4.2.6}$$

Rotor side :

$$V_r = R_r i_r + \frac{d\Psi_r}{dt} + j\omega_r \Psi_r \tag{4.2.7}$$

$$V_{dr} = R_r i_{dr} + \frac{d\Psi_{dr}}{dt} - \omega_r \Psi_{qr} \tag{4.2.8}$$

$$V_{qr} = R_r i_{qr} + \frac{d\Psi_{qr}}{dt} + \omega_r \Psi_{dr} \tag{4.2.9}$$

Similarly, the flux equations are as follows in 4.2.10:

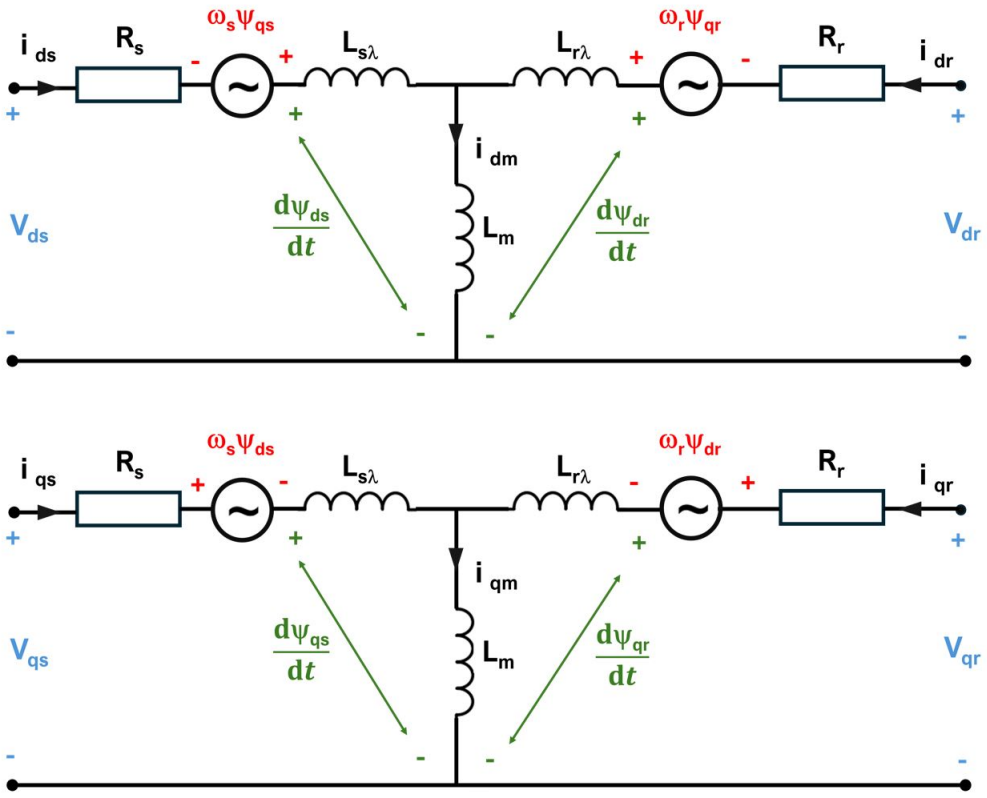

Figure 4.10: dq representation of DFIM circuit

Stator side:

$$\Psi_s = L_s i_s + L_m i_r \tag{4.2.10}$$
$$\Psi_{ds} = L_s i_{ds} + L_m i_{dr} \tag{4.2.11}$$
$$\Psi_{qs} = L_s i_{qs} + L_m i_{qr} \tag{4.2.12}$$

Rotor side:

$$\Psi_r = L_m i_s + L_r i_r \tag{4.2.13}$$
$$\Psi_{dr} = L_m i_{ds} + L_r i_{dr} \tag{4.2.14}$$
$$\Psi_{qr} = L_m i_{qs} + L_r i_{qr} \tag{4.2.15}$$

where,

$$L_s = L_{s\lambda} + L_m \tag{4.2.16}$$
$$L_r = L_{r\lambda} + L_m \tag{4.2.17}$$

4.2.3.3 DFIM: Γ-model

The T-equivalent circuit, however, is not suitable for control purposes since it is over parameterized due to the presence of one extra leakage inductance. For a conventional induction machine, the solution to this problem is to transform this circuit into the inverse-Γ model wherein, the rotor leakage inductance is removed. This allows for controller design with stator current and rotor flux as control parameters. However, for the DFIM where the objective is to control rotor current and stator flux, it is desired to use the Γ model wherein, the stator leakage inductance is removed. This allows for controller design with rotor current and stator flux as control parameters.

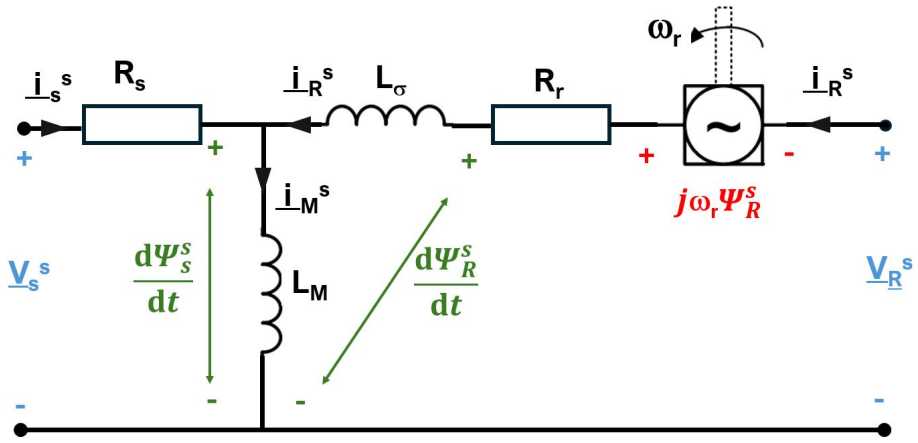

Figure 4.11: Γ-model of DFIM for rotor control

Equations in stator coordinates:

$$\mathrm{v}_s^s = R_s i_s^s + \frac{d\Psi_s^s}{dt} \tag{4.2.18}$$

$$\mathrm{v}_R^s = R_R i_R^s + \frac{d\Psi_R^s}{dt} - j\omega_r \Psi_R^s \tag{4.2.19}$$

where superscript s indicates stator coordinates. The model can also be described in synchronous coordinates as:

$$\mathrm{v}_s = R_s i_s + \frac{d\Psi_s}{dt} + j\omega_s \Psi_s \tag{4.2.20}$$

$$\mathrm{v}_R = R_R i_R + \frac{d\Psi_R}{dt} + j\omega_r \Psi_R \tag{4.2.21}$$

The stator flux, rotor flux, and electromechanical torque are given by:

$$\Psi_s = L_M(i_s + i_R) \tag{4.2.22}$$

$$\Psi_R = (L_M + L_\sigma) i_R + L_M i_s = \Psi_s + L_\sigma i_R \tag{4.2.23}$$

$$T_e = 3n_p \mathrm{Im}[\Psi_s i_R^*] \tag{4.2.24}$$

The parameters and quantities of the T- equivalent form relate to the Γ-model are defined based on the conversion factor γ and their relations are as follows:

$$V_R = \gamma V_r \tag{4.2.25}$$

$$i_R = \frac{i_r}{\gamma} \tag{4.2.26}$$

$$\Psi_R = \gamma \Psi_r \tag{4.2.27}$$

$$\gamma = \frac{L_{s\lambda} + L_m}{L_m} \tag{4.2.28}$$

$$R_R = \gamma^2 R_r \tag{4.2.29}$$

$$L_M = \gamma L_m \tag{4.2.30}$$

$$L_\sigma = \gamma L_{s\lambda} + \gamma^2 L_{r\lambda} \tag{4.2.31}$$

4.3 DFIM: Control

This section discusses the control strategies which were developed and in the literature review there were a lot of control strategies as shown in these research papers [7][9][13][15][27] and sensorless operation in [20]. There are various control strategies discussed for the DFIM, but field-oriented control is being used in this thesis. In this study, stator flux orientation is done based on the alignment of the rotor currents, and to control the rotor currents, we employ field-oriented control.

4.3.1 Field-oriented control

Field-oriented control is done to get high precision control over the torque and speed of the electric machines. It is particularly very important in AC machines like DFIM. Field-oriented control makes the controls easy by transforming non-linear complex systems to simpler linear systems, making the AC machines simpler and easier to control like the DC motor.

In field-oriented control or vector control there is the use of mathematical transformations like the Clarke and Park transformations, the three-phase AC currents are split into two orthogonal components (d & q). The d-component (direct axis) controls the magnetic flux, while the q-component (quadrature axis) controls the torque. By independently controlling these two components, precise control over the motor's torque and flux can be achieved.

In stator flux orientation, the reference frame is aligned with the stator flux vector. The stator flux is either measured directly using sensors or estimated from the machine's electrical parameters and measurements of stator voltages and currents. The rotating dq reference frame aligned with the stator flux vector is obtained by transforming the stator current and voltage vectors using the transformation angle, which is usually the angle difference between the stator flux and the rotor flux. This makes the d-axis aligned with the stator flux. The torque output is controlled by the q-component of the current, which can be adjusted independently of the stator flux. The torque may be controlled independently of the stator flux because the d-component of the current is aligned with the stator flux and directly controls the stator flux magnitude. Hence, the decoupled control of flux and torque is possible through field-orientated control.

To align the dq currents to the stator flux vector, the stator flux has to be estimated first or it has to be measured using sensors. In the case of stator flux estimation, it is done based on the three-phase stator voltages which are then transformed to synchronous $\alpha\beta$ coordinates using Clarke transformation as shown in 4.3.1.1. Later once the dq reference currents or voltages are found through the current control algorithm, the inverse park transformation is used to get the

three-phase voltages to be fed to the converter on the rotor side of the machine. In this thesis, as the converters as considered to be ideal transfer blocks, it is not included, instead the currents are directly fed through the rotor windings as depicted in 4.3.4. The field-oriented control enhances the dynamic response and efficiency of the machine's control system. As the control adapts to variable speeds, it is very useful in the case of a double-fed induction machine where there is variable speed most of the time.

4.3.1.1 Flux orientation and flux estimation algorithm (Based on equation 4.2.18)

The stator flux of DFIM is calculated based on the three-phase voltages (V_s^s) and currents (i_s^s) from the stator and the magnitude of stator resistance (R_s). In this model, field-oriented control is implemented, wherein a flux linkage must be aligned with the reference frame 4.7. The stator-flux oriented system is the method by which the rotor currents are controlled in this study.

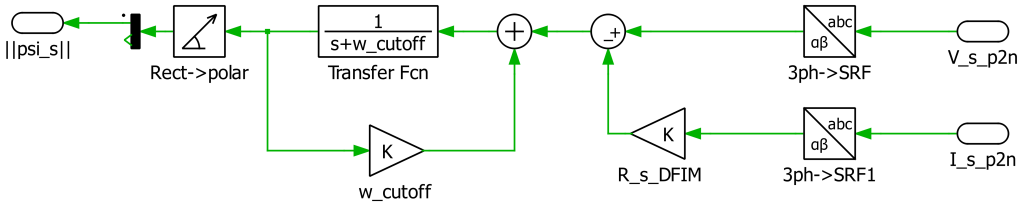

Figure 4.12: Schematic of Flux estimation algorithm

4.3.1.2 Slip angle calculation

The slip angle is essentially the difference between the stator flux and the rotor flux. In the model, it is done as shown in Fig. 4.13. Here, the slip frequency (ω_{slip}) is calculated and integrated to get θ_{slip} which is the transformation angle used to convert the reference currents from Sec. 4.3.2 in $'d-q'$ reference frame to $'abc'$ reference frame currents which are being fed to the rotor end of the DFIM in Sec. 4.3.4.

$$\omega_{slip} = \omega_s - \omega_r \tag{4.3.1}$$

$$\theta_{slip} = \theta_{\varphi s} - \theta_{\varphi r} \tag{4.3.2}$$

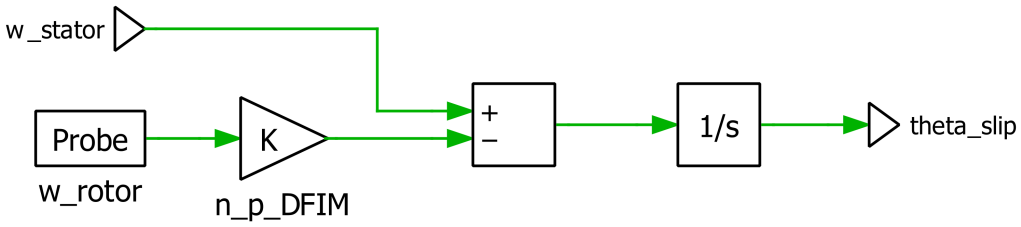

Figure 4.13: Schematic of slip angle calculation

4.3.2 Torque control and Reactive power control

While the d component of the rotor current can be used to control the reactive power at the stator terminals, the q component of the rotor current controls mainly the produced torque for both

reference frames. The current controller usually has current references as an input and three-phase voltages as the output. In this study, the current controller is considered to be ideal. Hence, the current references are directly fed to the rotor winding side as inputs.

The electromechanical torque is given by :

$$T_e = \frac{3}{2} n_p \mathrm{Im}[\Psi_s \mathrm{i}_R^*] \approx -\frac{3}{2} n_p \psi_s i_{Rq} \tag{4.3.3}$$

The torque can be controlled by the q component of the rotor current, i_{Rq} and since it is difficult to measure the torque, it is usually controlled in an open loop. Thus, the torque control logic for the calculation of q current reference i_{Rq}^* is employed using the reference torque, T_e^{ref} and the flux estimated ($\hat{\psi}_s$) in 4.3.1.1.

$$i_{Rq}^* = -\frac{2T_e^{ref}}{3n_p\hat{\psi}_s} \tag{4.3.4}$$

For a stator-flux oriented system, the reactive power control logic to get the d current reference component i_{Rd}^* is given by equation 4.3.5 considering that the DFIM can be operated at unity power factor by controlling the rotor currents and is shown in Fig. 4.14.

$$i_{Rd}^* = \frac{\hat{\psi}_s}{\hat{L}_M} \tag{4.3.5}$$

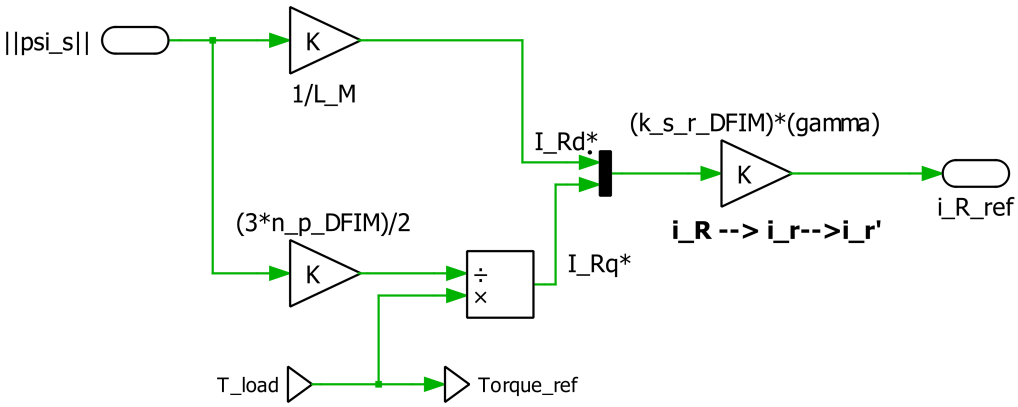

Figure 4.14: Schematic of current references calculation

4.3.3 Driver inputs & Machine model

4.3.3.1 Driver inputs: References

The DFIM output (T_e) is dependent only on the torque demand ($T_{e,ref}$) which is fed through the 'References' block. This $T_{e,ref}$ is used for i_{Rq}^* calculation as part of the torque control logic.

In addition, the references block gives the information about the load torque (T_{load}) which is computed based on the speed profile demanded. The speed controller logic is used to compute

T_{load}, as discussed in the next section. For the purpose of this thesis, multiple drive cycles are used to analyze the performance of the DFIM under varying operating conditions

4.3.3.2 Machine model

The load torque to the electric machine is estimated based on the reference speed through a speed controller. The speed reference is considered to be the speed profile of the PMSM machine output which the DFIM has to follow.

An actuator is included in the machine model, which directs the DFIM machine's speed to a specific value based on the speed of the PMSM machine. The torque reference obtained from the speed reference is sent to the DFIM as load torque after passing through a speed controller.

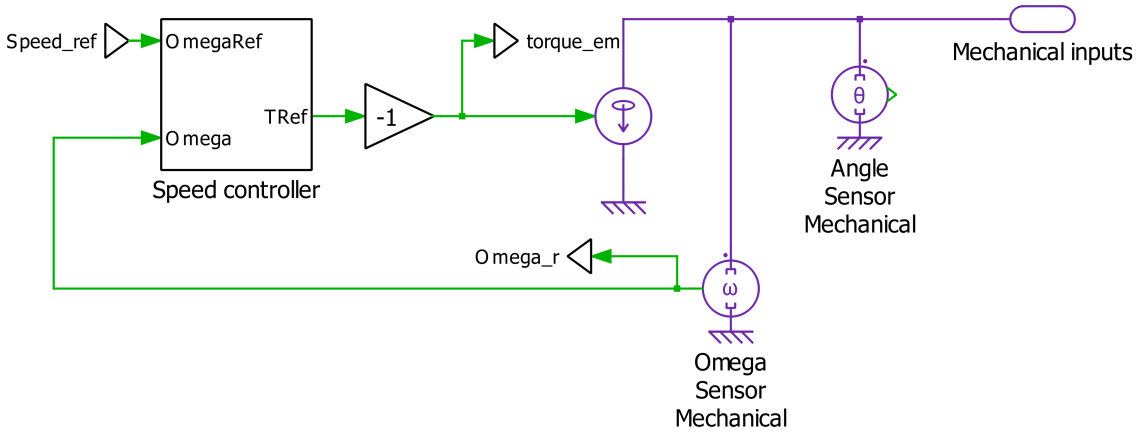

Figure 4.15: Schematic of machine model

The machine model (as discussed in Sec. 2.2.1) feeds the rotor speed and rotor position information to the DFIM machine. In addition, it also contains the speed controller which dictates the load torque based on the speed profiles fed through the references.

The speed controller is defined by the following transfer function:

$$G(p) = \frac{\omega_r(p)}{T_e^{ref}(p))} = \frac{1}{\frac{J}{n_p}p + B_a} \tag{4.3.6}$$

where, B_a: active damping (in this case, it is frictionless, hence zero). For this controller, the k_p and k_i values are calculated according to the following equations with a controller bandwidth of $\alpha_s = 100$Hz, $B = 0$, $k_w = 0.1$.

$$k_p = \alpha_s.J \tag{4.3.7}$$

$$B_a = k_p - B \tag{4.3.8}$$

$$k_i = \alpha_s.(B_a + B) \tag{4.3.9}$$

4.3.3.3 Reference Speed and Torque

The reference speed and torque can be any load and torque point that the PMSM operates at, during the complete driving cycle. In this study, the WLTC cycle (4.16, 4.17), repeated acceleration profile (4.18, 4.19) and constant speed and torque points were used to observe the behaviour of the DFIM.

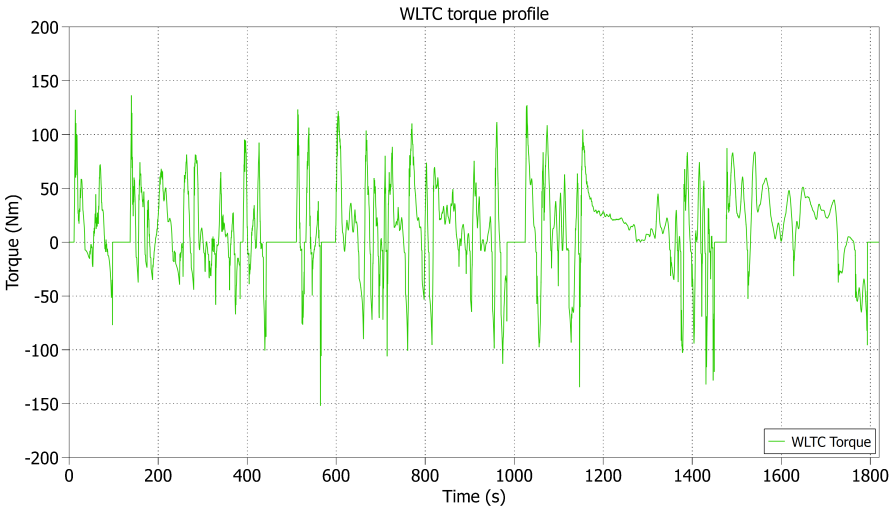

Figure 4.16: WLTC torque profile

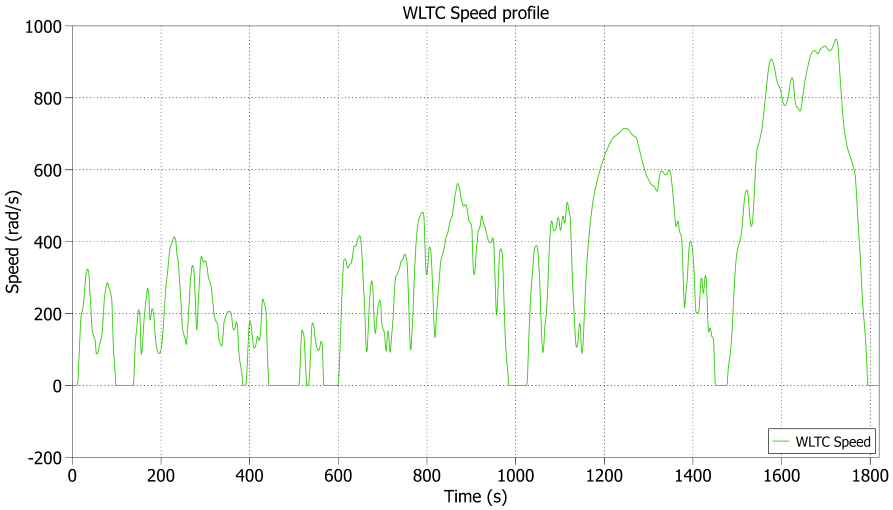

Figure 4.17: WLTC speed profile

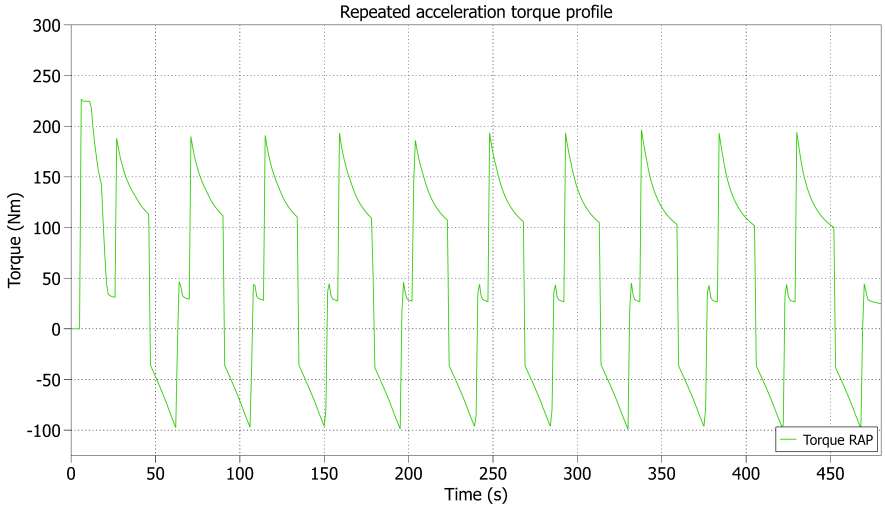

Figure 4.18: Repeated acceleration torque profile

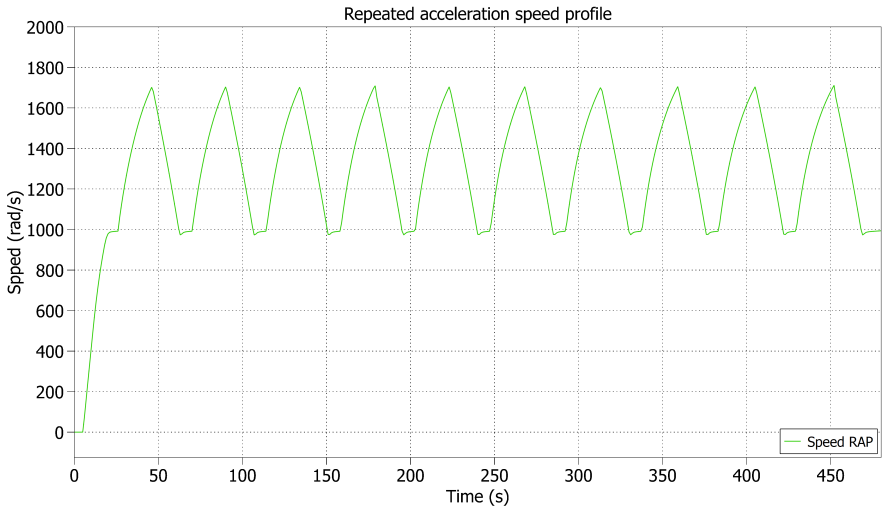

Figure 4.19: Repeated acceleration speed profile

4.3.4 Current transformation block (dq-abc)

The reference currents obtained from the Sec. 4.3.2 are transformed from dq to abc currents in this block. The transformation angle used is θ_{slip} from Sec. 4.3.1.2. These currents are then fed to the rotor side of the DFIM.

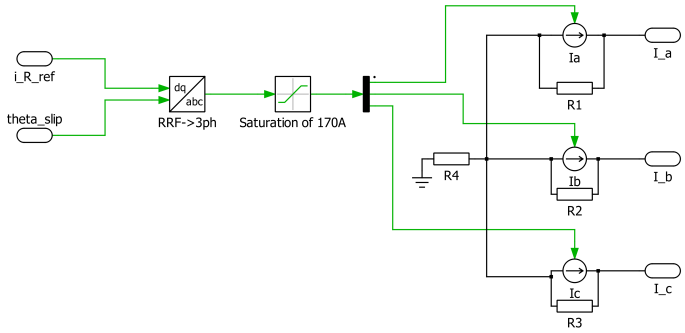

Figure 4.20: Schematic of current transformation block

5

Results and Discussions

The focus of this chapter is on the analysis of the DFIM model discussed in previous chapters under steady state and standard operating conditions. Since the purpose of this thesis is to understand the feasibility of using a DFIM as the front wheel drive in an all-wheel drive setup, the performance analysis is done based on multiple parameters ranging from voltage & current requirements to power & efficiency of the model. These results and discussions are to be considered, keeping in mind the assumptions and limitations enlisted in chapter 2 of the report for a transparent and thorough understanding of the discussion of results in this chapter.

5.1 T-ω envelop

The first and foremost requirement to conduct any analysis is to establish the operating range of the DFIM in terms of torque (T) and speed (ω). Since there is no physical machine available, to establish this envelop, a sweep is conducted using a torque ramp for multiple speeds at regular intervals. Since the controller is an open loop type defined by the torque control objective, any torque requested can be achieved by the model. However, this cannot be achieved while also maintaining the speed, which can be seen as shown in Fig. 5.1.

The torque corresponding to the point at which there is speed deviation is the maximum torque that can be achieved at the said speed. For instance, in Fig. 5.1, it can be seen that for a speed of 7000 RPM, the maximum torque that can be achieved using the subject DFIM is $\sim$234 N-m. By performing this exercise over the whole speed range, both in the positive and negative torque regions, we could come up with the T-ω envelop as shown in Fig. 5.2.

The locus of the data points shown in blue represents the maximum positive torque envelop (in motor mode), while that in red represents the maximum negative torque envelop (in regeneration mode). These data points are listed in table A.1. In the coming sections, this envelop is used to conduct a steady state analysis to understand and assess the performance of the DFIM in terms of power requirements at the stator & rotor ends, efficiency, and rotor excitation (voltage and current).

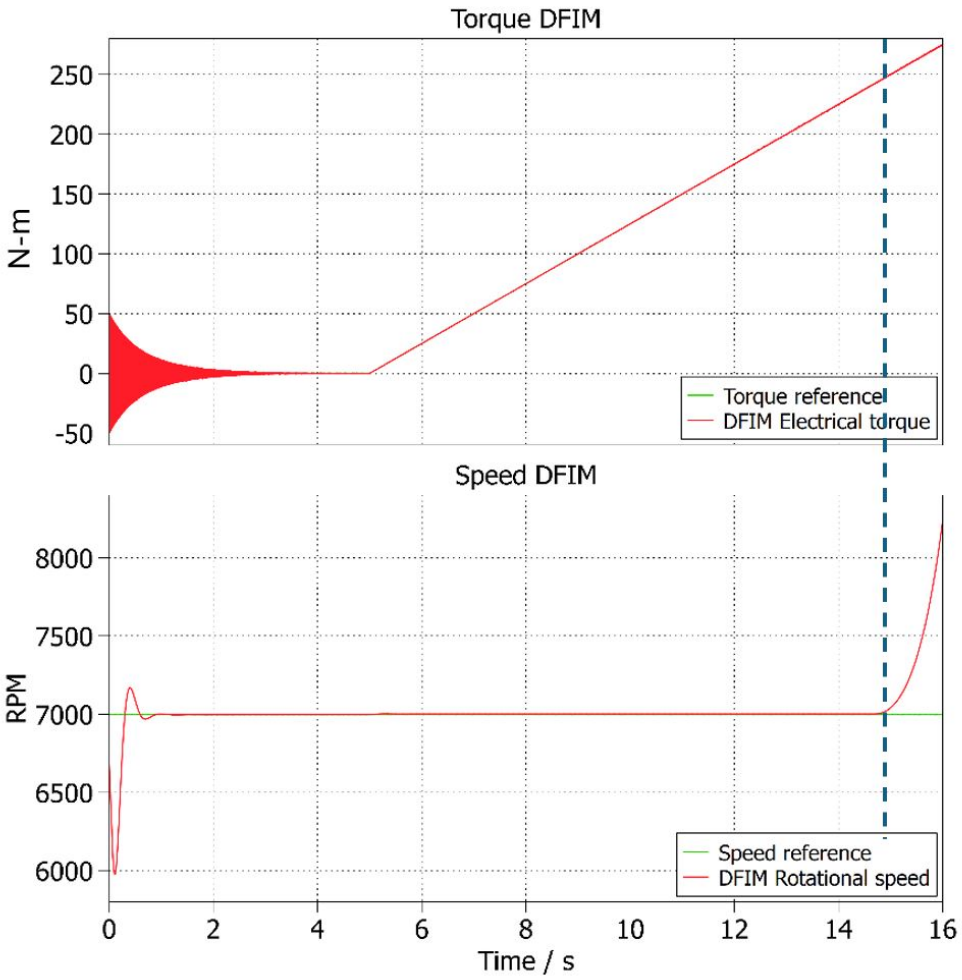

Figure 5.1: Plot showing the maximum achievable torque for a given speed (e.g. 7000 RPM)

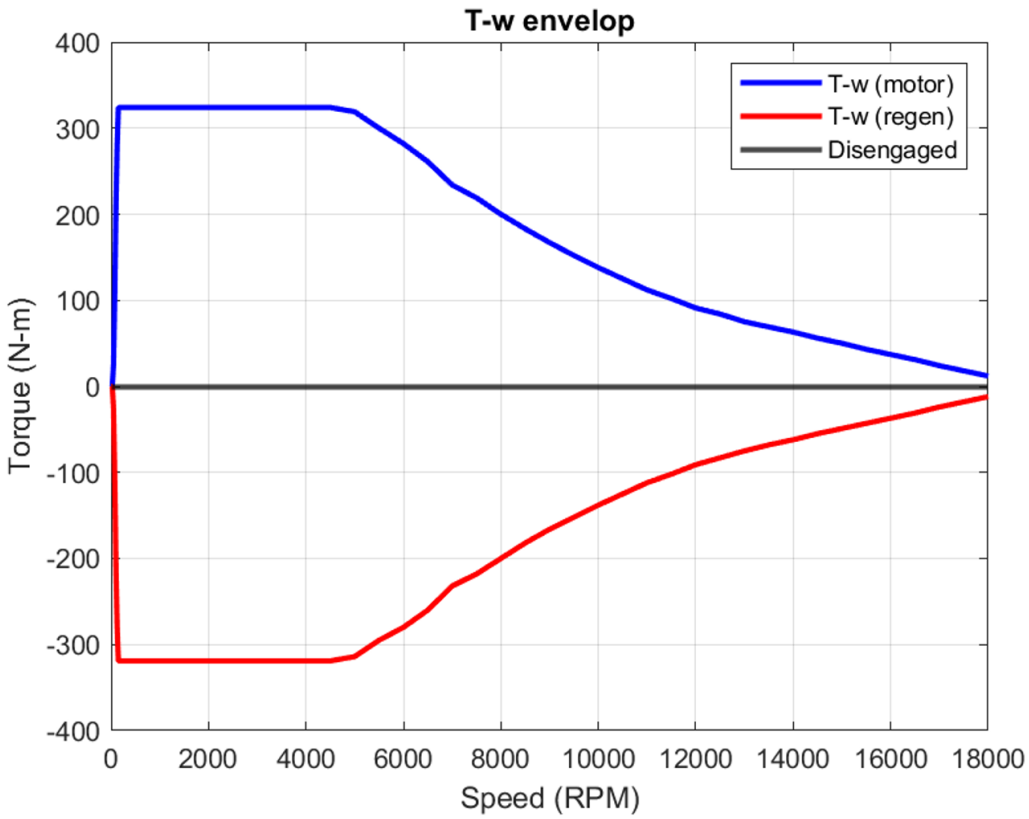

Figure 5.2: T-ω envelop obtained in both motor and regen mode

5.2 Performance analysis in steady state

A steady-state analysis is conducted to understand the workings of the DFIM in a controlled manner. To conduct this steady state analysis, a drive cycle is developed that covers all the possible torque and speed combinations, and each of these combinations is run for 10 seconds each to ensure that the steady state is achieved. Once the steady state is achieved, the different metrics for performance assessment are calculated and analyzed.

5.2.1 T-ω sweep: custom drive cycle

To ensure that all the combinations of torque and speed combinations are covered, a custom drive cycle is derived from the T-ω sweep plot as shown in Fig. 5.3.

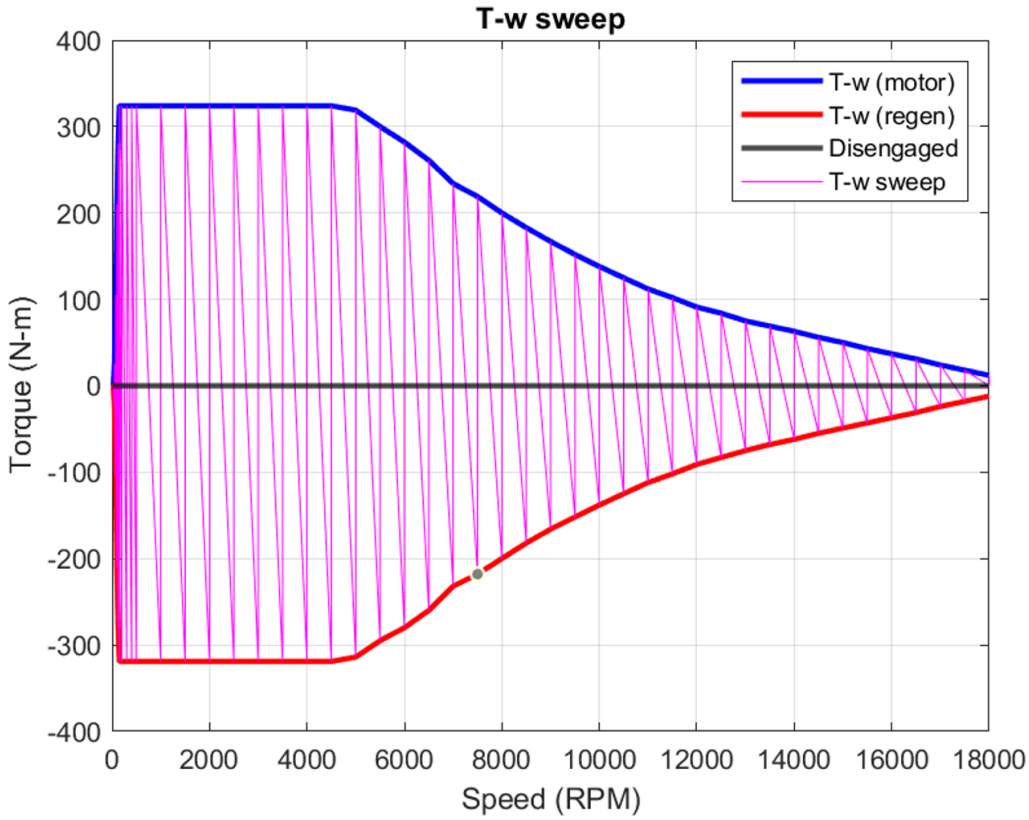

Figure 5.3: T-ω sweep drive cycle as shown on the T vs ω plot

Converting the above T-ω sweep into a time series, a drive cycle that lasts for a duration of about 18090 seconds is generated as shown in Fig. 5.4. It is also to be noted that Fig. 5.4 depicts both torque-speed profiles requested, and torque-speed profiles achieved. This shows that the controller is functioning as intended and so, the results obtained are reliable within the confines defined by the assumptions and limitations.

5.2.2 Voltage & Current: stator and rotor requirements

The voltage and current requirements of the stator and rotor are important metrics to assess the feasibility of the DFIM-driven AWD model. It is necessary to have these requirements within the limitations dictated by the power electronics to be able to adopt DFIM into existing all-wheel drive architecture which involves choosing appropriate inverter topology as well. For preliminary

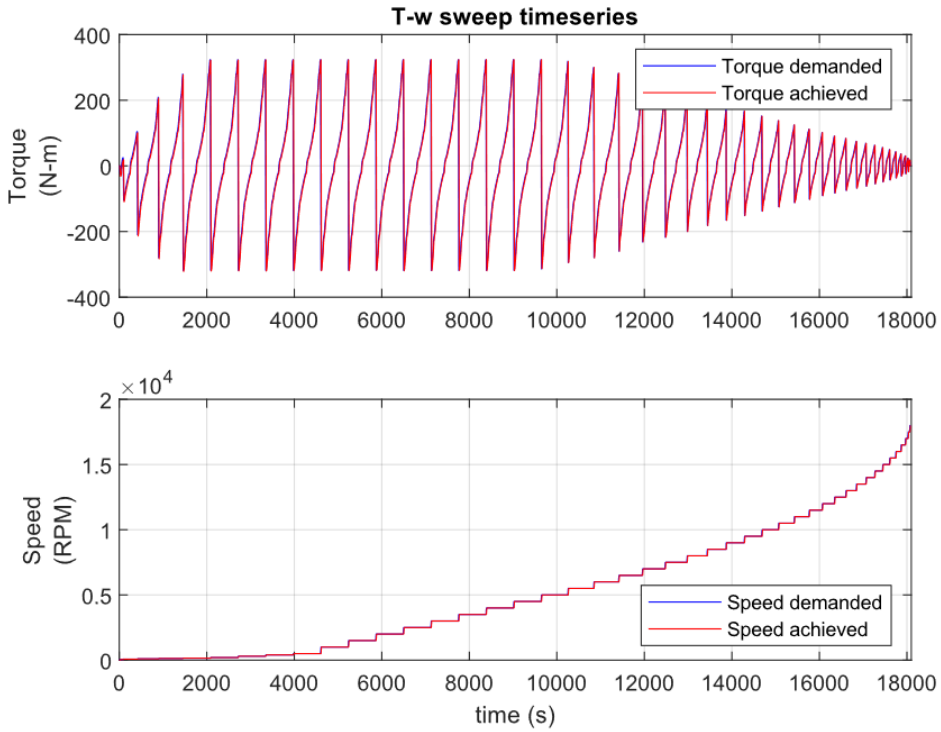

Figure 5.4: T-ω sweep drive cycle represented as a time series and compared with speed and torque profiles achieved

assessment, it is decided to have the rotor current limited to ∼12A to 15A and total rotor excitation power limited to ∼6kW (approximately 1-3% of the stator power consumption).

From Fig. 5.5 for maximum stator voltage of 1000V, the rotor voltage is a maximum of ∼72V at t= 2000s which corresponds to a torque- speed combination of 320N-m at 500RPM (refer Fig. 5.4). This combination of torque and speed is an extreme operating case and can be argued that the rotor excitation voltage can be limited to under 40V for most cases (this can be seen in greater detail in later sections with standard drive cycles).

This finding can be further observed in Fig. 5.6 which shows a contour plot of both stator and rotor voltages for a whole range of torque and speed combinations. It can be observed in Fig. 5.6 that stator voltage increases with speed as defined and described in chapter 4. Consequently, the rotor excitation voltage varies proportional to the torque demanded. It can be seen that the rotor excitation voltage is around 20V for ±100N-m and 40V for ±200N-m. Thus for the purpose of development of the DFIM-driven all-wheel drive, a 40V rotor excitation voltage is sufficient. This results in a much smaller micro-converter with compact power electronics compared to the existing all-wheel drive with an independent and more complex inverter topology for induction motor control.

Similarly, Fig. 5.7 compares the stator and rotor current requirements for various torque-speed requirements. It can be noted from Fig. 5.7 that, the stator and rotor current requirements vary with torque demand. Also, the ratio of stator and rotor currents follow the stator to rotor turns ratio, as expected. This validates the accuracy of the model and further reinstates the confidence in the model's results. The maximum current requirement at the stator and rotor are ∼180A and ∼70A respectively for a torque demand of about 320 N-m. Similarly, the stator and rotor current requirements at torque of 100 N-m and 200 N-m are (∼80A, ∼30A) and (∼120A, ∼50A) respectively. Thus for all practical applications of the machine, the MOSFET ratings of power electronic components are within the acceptable ranges of 180A as is followed currently.

In Fig. 5.8 & 5.9, we can get a much clearer picture of what the d and q-axis components

(stator flux oriented frame of reference) of voltages and currents of the stator and rotor. It is to be noted that the d-components of these parameters are almost non-existent due to the fact that this is a steady state analysis and in a steady state, the slip between stator and rotor fluxes is almost zero, a key distinguishing feature of the double-fed induction machine.

In addition, it is also to be noted that the current requirements are the least at extremely high speeds and low torque demands. This behaviour is commensurate with the observations to be made in further sections which discuss the power requirements (stator, rotor, and mechanical) and efficiency.

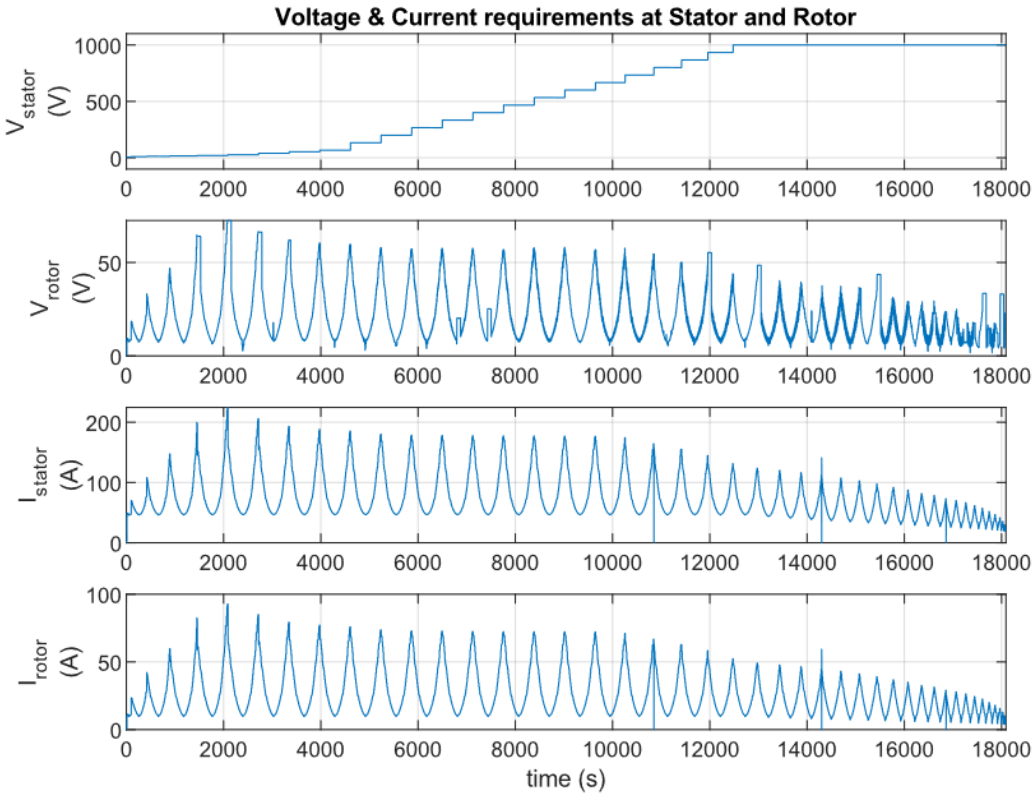

Figure 5.5: Voltage and current requirement at the stator and rotor in response to the T-ω sweep drive cycle

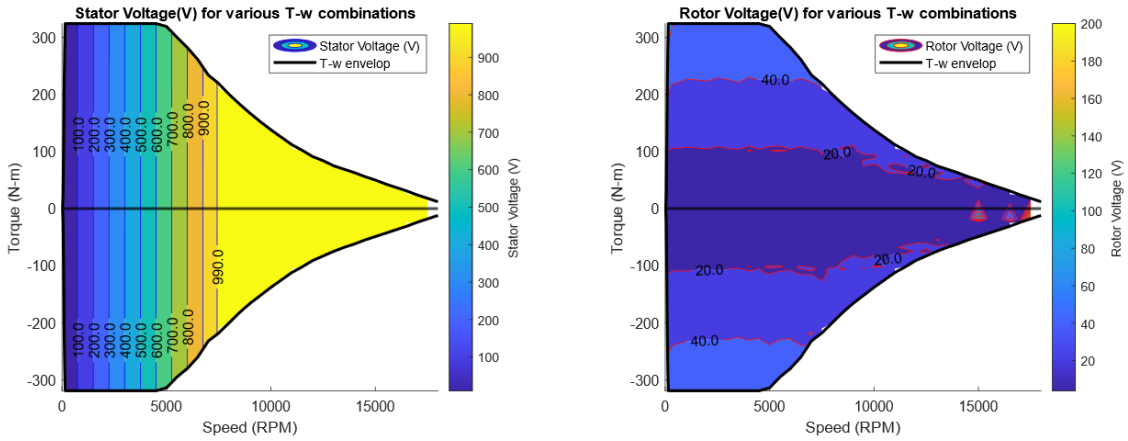

Figure 5.6: Voltage requirement contours for stator and rotor within the T-ω envelop

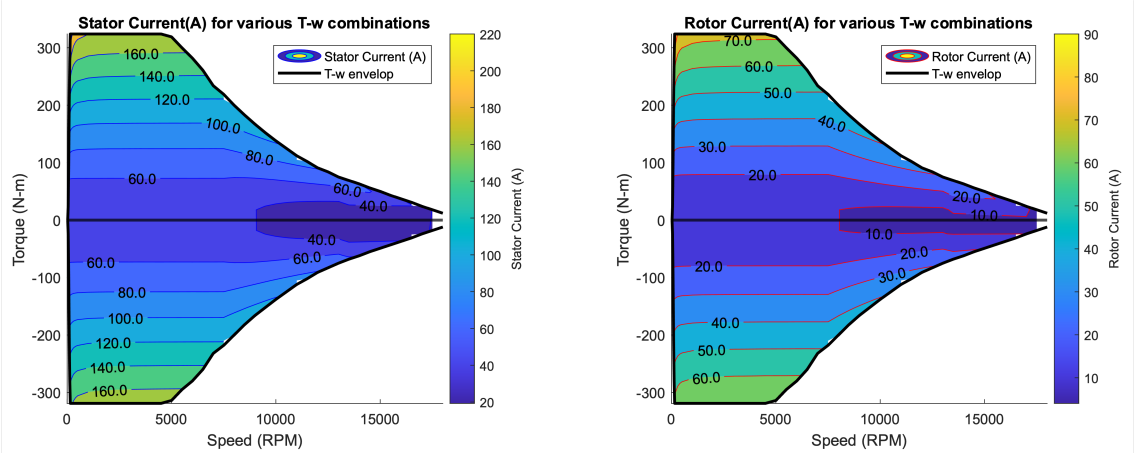

Figure 5.7: Current requirement contours for stator and rotor within the T-ω envelop

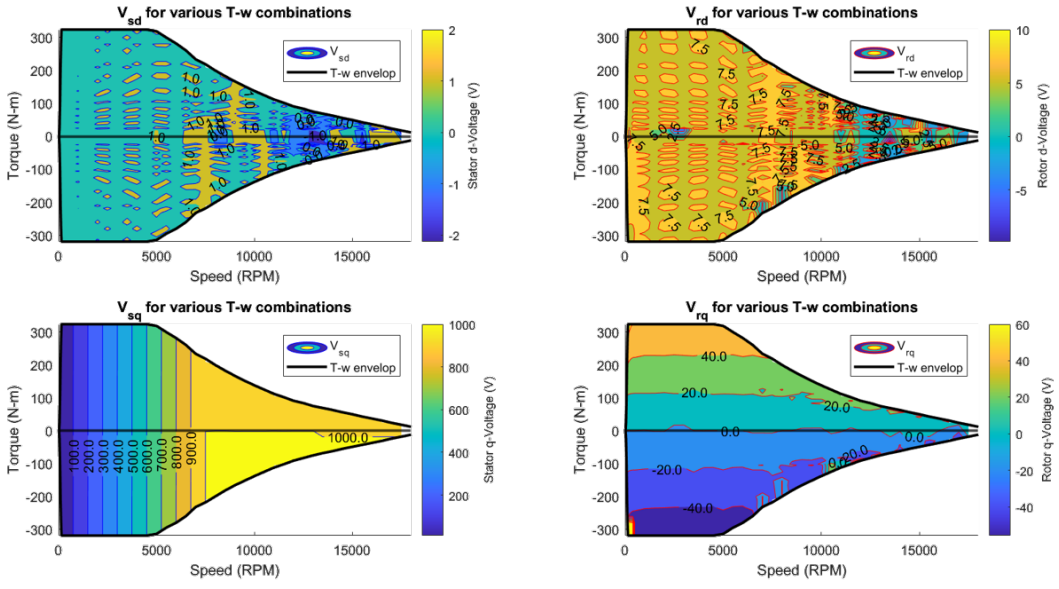

Figure 5.8: d-q Voltage components (stator flux oriented frame of reference) at stator and rotor

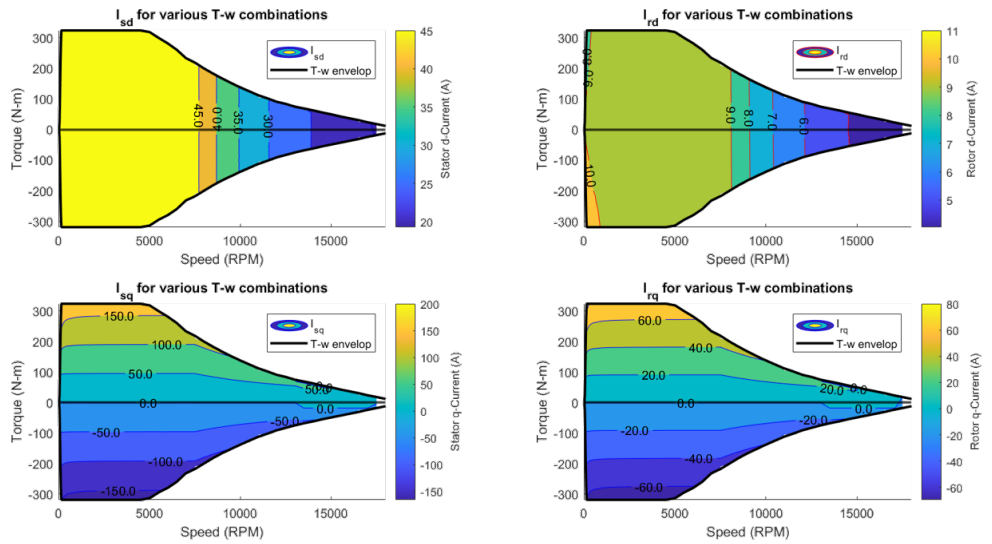

Figure 5.9: d-q Current components (stator flux oriented frame of reference) at stator and rotor

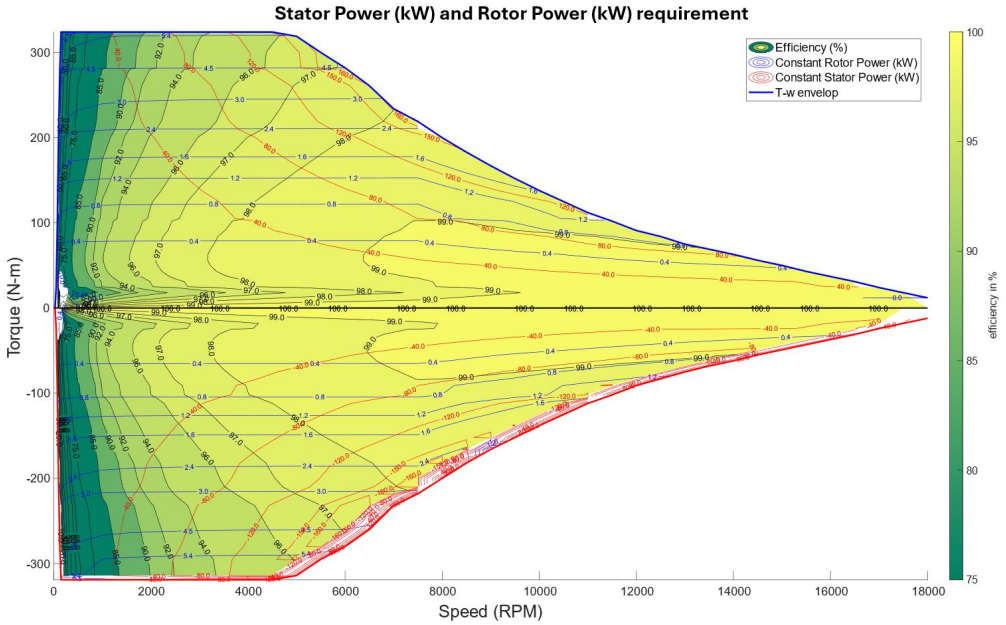

Figure 5.10: Composite contour plot depicting efficiency and power requirement at stator and rotor

5.2.3 Power & Efficiency

This section discusses the performance of the DFIM in steady-state conditions for different torque-speed combinations in terms of stator power, rotor power mechanical power, and efficiency. For this purpose, calculations are carried out as follows:

$$P_m = T * \omega \tag{5.2.1}$$

$$P_{stator} = Re(v_s * i_s) \tag{5.2.2}$$

$$P_{rotor} = Re(v_r * i_r) \tag{5.2.3}$$

$$\eta_{DFIM} = \frac{P_m}{P_s + P_r} * sign(P_m) \tag{5.2.4}$$

By carrying out these calculations for various combinations of torque speed across the T-ω envelop, a composite plot as shown in Fig. 5.10 is generated showing efficiency, contour lines of stator & rotor powers. For this analysis, it is important to note that this analysis assumes ideal power electronics and thus, these numbers can vary accordingly. This implies that the only losses considered in this analysis are machine losses i.e., resistive losses and inductive losses.

From this plot, the following information can be extracted. Firstly, this composite plot has information about the efficiency across the torque-speed range, represented as a contour plot. Notably, the efficiency of the machine is upwards of 90% for speeds above 2000 RPM and efficiency improves with less torque demands and high speeds.

Secondly, the plot has information about stator power and rotor power usage represented as constant power lines (represented in red and blue respectively). From this plot, it can be seen that, the maximum stator power consumption is around 160 kW in magnitude and as a general trend, the stator power consumption increases with increasing proximity of the torque-speed combination to the T-ω envelop.

Similarly, the constant rotor power lines have a magnitude increasing with torque demanded. As a general trend, the constant rotor power lines have a similar profile as the T-ω envelop, i.e., the rotor power is constant with respect to torque demand until a speed range. Then, for the same rotor excitation power, the achievable torque demand is reduced.

Thus, this composite plot, shown in Fig. 5.10, can be used to optimise the rotor excitation requirements depending on the torque and speed requirements to achieve the best possible efficiency.

5.3 Performance in Transient operation

5.3.1 Slip in transient operation

Before studying the transient behaviour of the DFIM in greater detail using specific drive cycles, it is important to highlight one key distinction between a regular Induction machine (IM) and the DFIM modelled throughout this thesis.

Unlike an induction machine which generates torque by maintaining a certain amount of slip throughout its operation, a DFIM operates (refer to Sec. 3.1) without any slip during steady state operation (in synchronous mode) and has slip during transient operation. This can be observed in Fig. 5.11 & 5.12, where the relation between slip and the corresponding effect on rotor voltage and current are depicted is clearly shown.

During transient operation i.e. between t=10s and t=15s, we see a ramp up of speed from 100 rad/sec to 150 rad/sec, which results in a slip frequency of $\sim$1 rad/sec i.e., approximately 1% of slip. This transition results in a sinusoidal behaviour of the rotor voltage and current components (refer to Fig. 5.12), which have constant behaviour before and after the transient behaviour. Since voltage is related to the rate of change of flux, it can be deduced that, during a steady state, where rotor voltage is constant, rate of change of rotor flux is constant. This is indicative of the fact that the angle (in other words, slope) of rotor flux in the d-q system defined by stator flux orientation is fixed and hence, slip is zero. This is however not the case in transient operation, where the rotor voltage varies sinusoidally. Thus by the same reasoning, it can be concluded that there exists a slip in transient operation. This is evident in Fig. 5.11 as well.

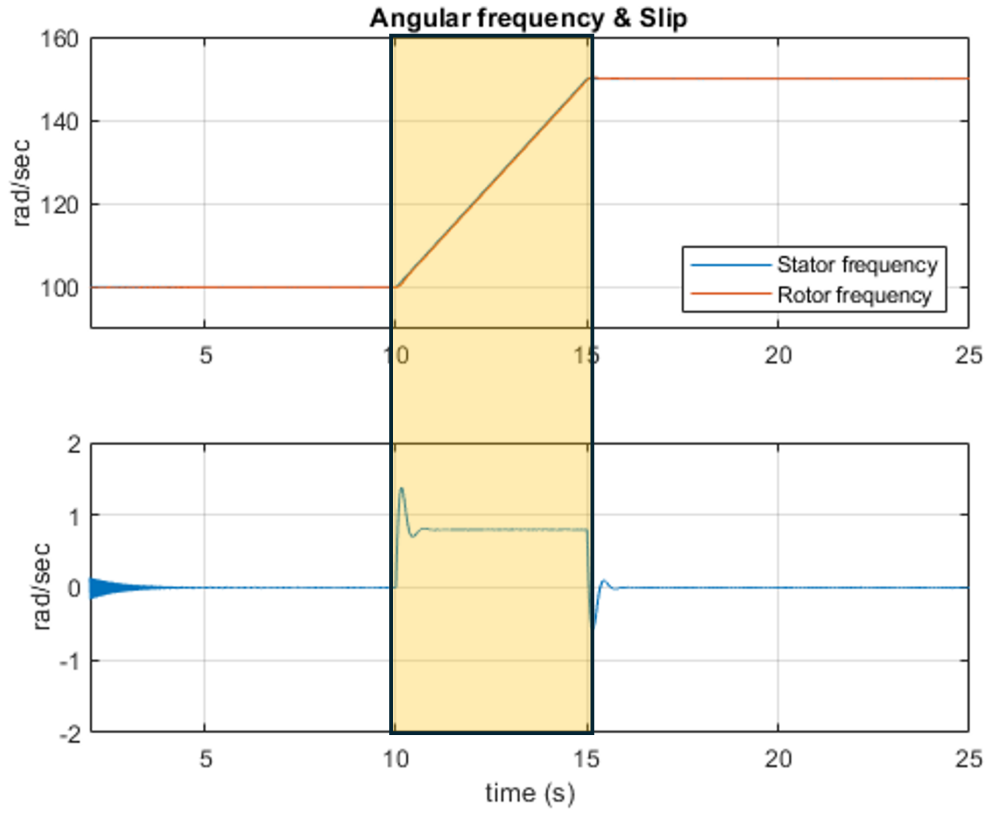

Figure 5.11: Controlled scenario of transient operation with slip between rotor and stator

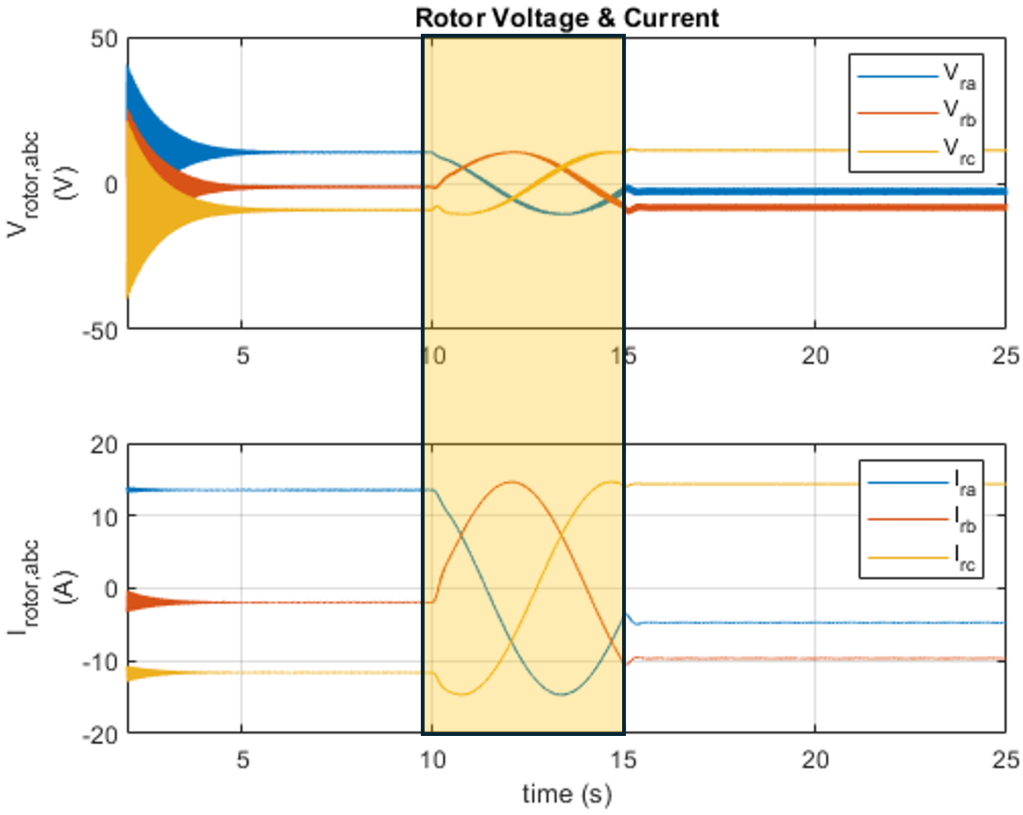

Figure 5.12: Effect of transient operation with slip on the nature of voltages and currents

In the coming sections of this chapter, the focus is going to be on analysing the transient behaviour under specific driving cycles including the WLTC and the repeated acceleration profile for analysis under specific driving conditions.

5.3.2 WLTC driving cycle

WLTC drive cycle represented on T-ω envelop:

The WLTC driving cycle is a very representative driving cycle that covers a lot of operating scenarios (as marked from A through F and colour coded in Fig. 5.13 & 5.14):

1. Driving modes:
   (a) Motor mode of operation (positive torque)
   (b) Regenerative mode of operation (negative torque)
2. Torque-speed combinations:
   (a) Low-speed range (A) and peak torque (around 140 N-m)
   (b) Medium speed range (B & C)
   (c) High speed range (D, E & F)
3. Sustained acceleration from zero speed to maximum speed (D)
4. Sustained high-speed operation (E)
5. Sustained deceleration from maximum speed to zero speed (F)

The same operation conditions can be seen in Fig. 5.14 using the colour coding. These operating conditions are the most frequently encountered scenarios and hence WLTC is the most representative drive cycle to test the DFIM performance.

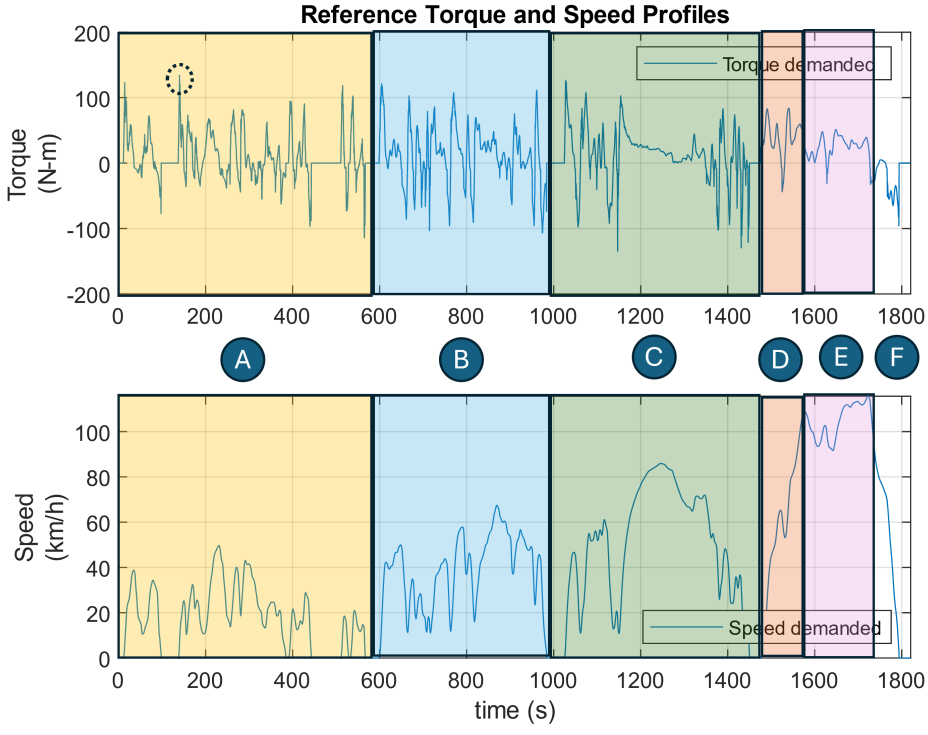

Figure 5.13: WLTC with clearly marked modes of operation and events

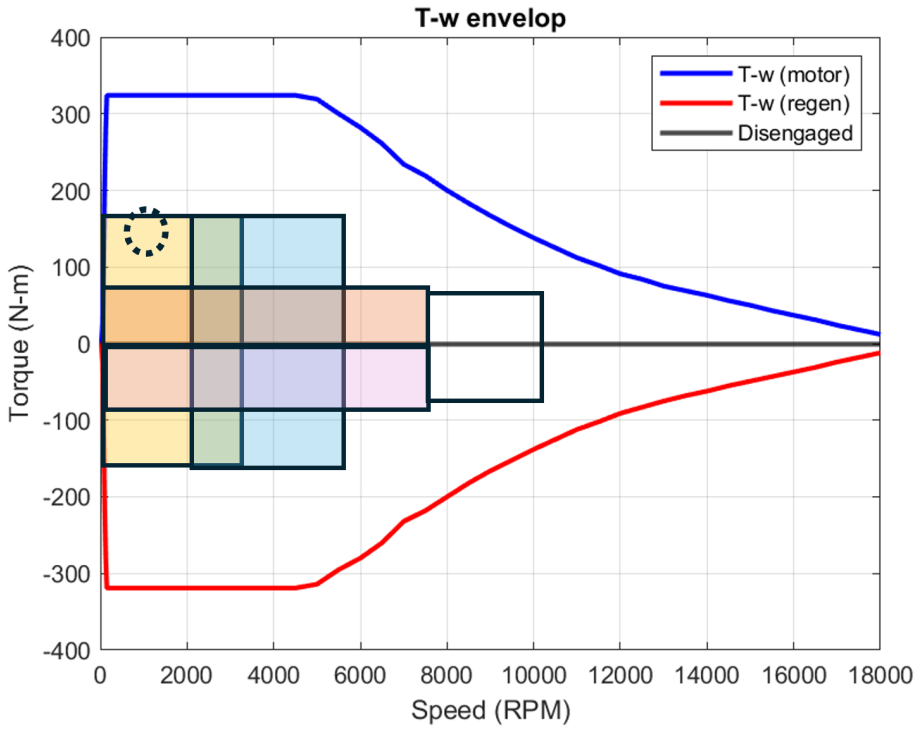

Figure 5.14: Representation of WLTC on the T vs ω plot

From Fig. 5.15, it can be seen that, the desired torque and speed output is achieved and hence, the result and inferences thus obtained are reliable and acceptable within the limits of the assumptions.

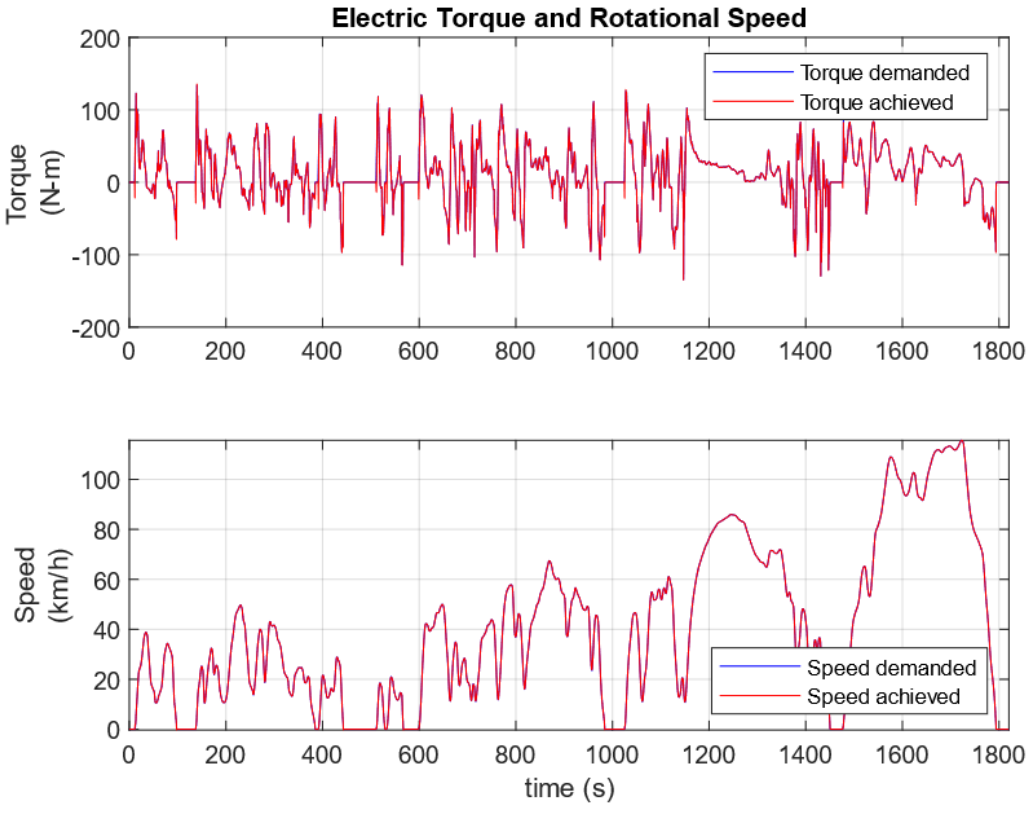

Figure 5.15: Plot showing the compliance of torque and speed profiles achieved with the WLTC drive cycle demanded

Voltage and Current profiles:

As it was established in previous chapters, one of the key focus of this study is to understand the variation of voltage and current requirements at the rotor for a variable frequency drive dictated by variable stator frequency, while operating within the power electronic requirements. To ensure that these conditions are met, it is important to show that the stator voltage varies as a function of the speed (and by extension, frequency) and within the pre-determined voltage limit of 800V. This can be visualised in Fig. 5.16, where stator voltage follows the speed profile and when the voltage requirement exceeds 800V, it is limited to 800V.

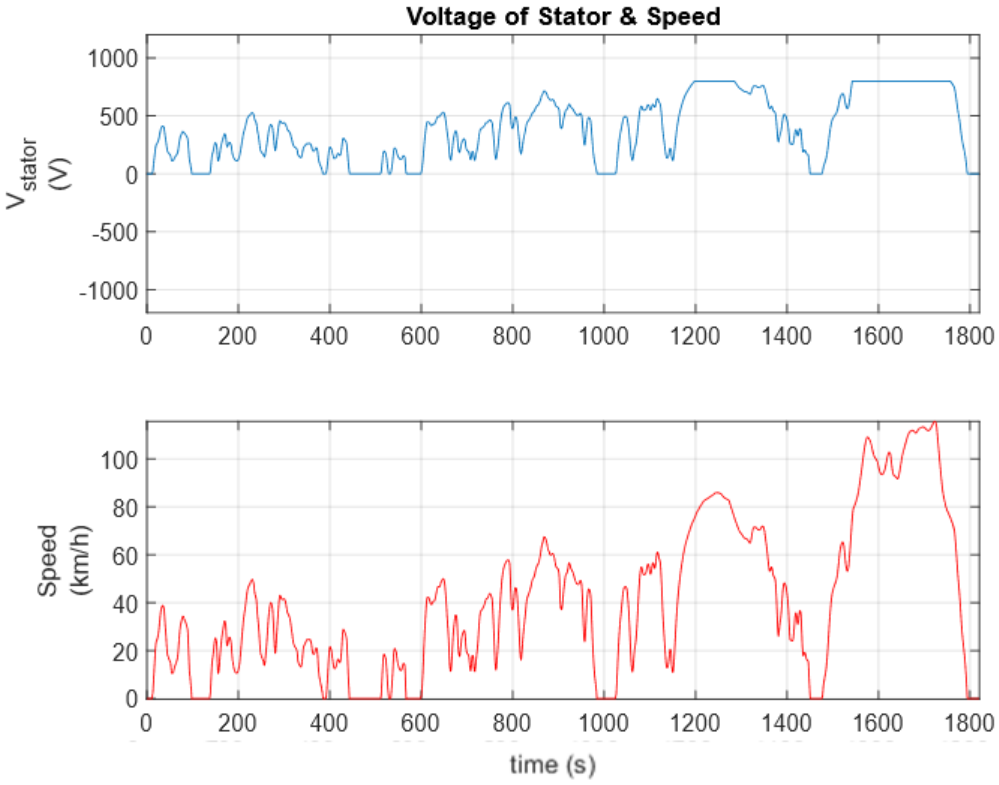

Figure 5.16: Figure depicting the linear relation between stator voltage and speed profile subject to voltage limitation

Similarly, it is notable from Fig. 5.17 that, the rotor current variation depends predominantly on torque demanded. This is evident in the Fig. 5.17, in which, it is shown that rotor q-current component profile matches that of the torque demand. This is especially true in the fact that, the frequency of the current component varies according to the variability of the torque demanded. For instance, this can be seen clearly in the time intervals as marked.

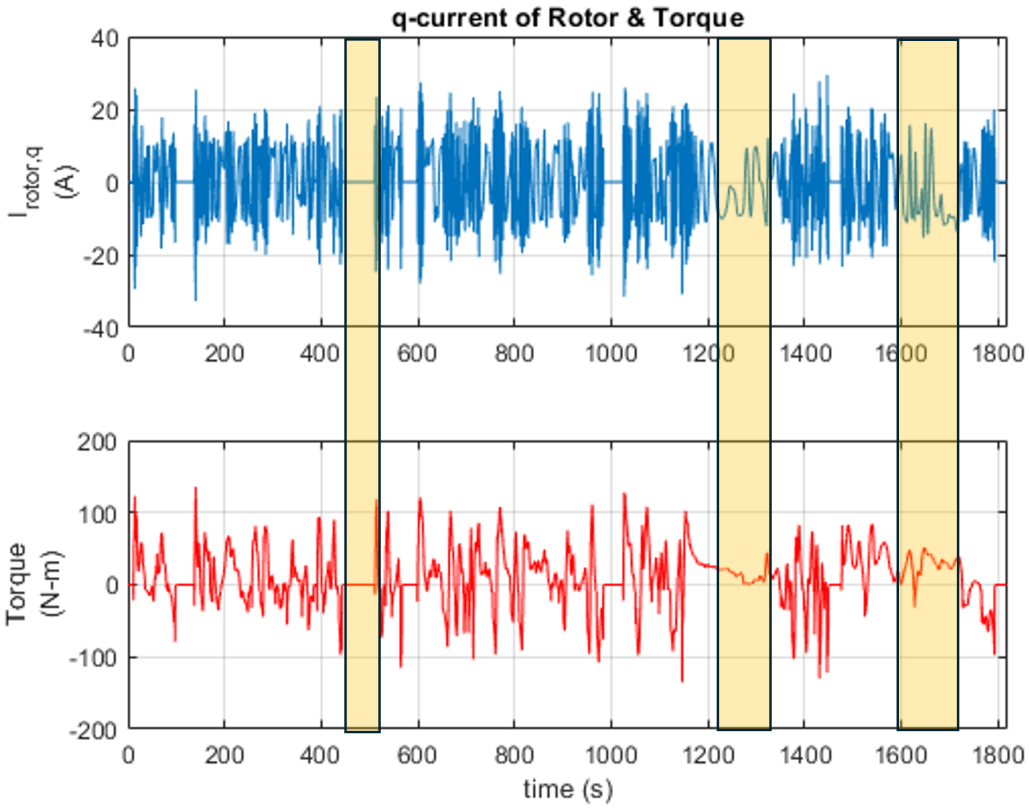

Figure 5.17: Figure depicting the relation between rotor q current and torque profile subject to voltage limitation

However, the rotor voltage shows instantaneous spikes in the data as shown in Fig. 5.18. These erroneous spikes are a result of computational limitations and could be neglected as they appear at transition points and bear no consequence as shown thus far. Having said that, disregarding the spikes, the rotor voltage is under 30V in general and hence within the acceptable power electronic limitations.

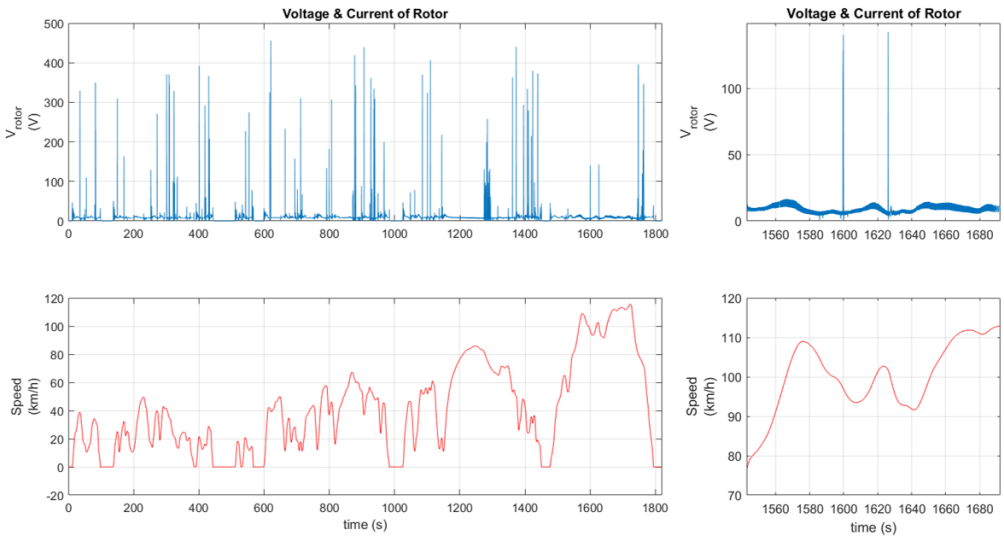

Figure 5.18: Plot showing the errors in rotor voltage due to computational limitations highlighting general compliance

Power and efficiency:

Fig. 5.19 shows that, for the complete WLTC cycle, the mechanical power consumption is within 50 kW range. And, it is notable that this power requirement is met primarily by the stator power consumption and the rotor power consumption is under 2kW (∼3% of stator power). This results in a very efficient drive with efficiency upwards of 90% as shown in the efficiency plot of Fig. 5.19. However, the computational errors in rotor voltage measurement, mentioned in the previous section are reflected in the calculation of efficiency as well. Thus there are instances where the efficiency appears to be extremely low. Thus, these disturbances are worth disregarding.

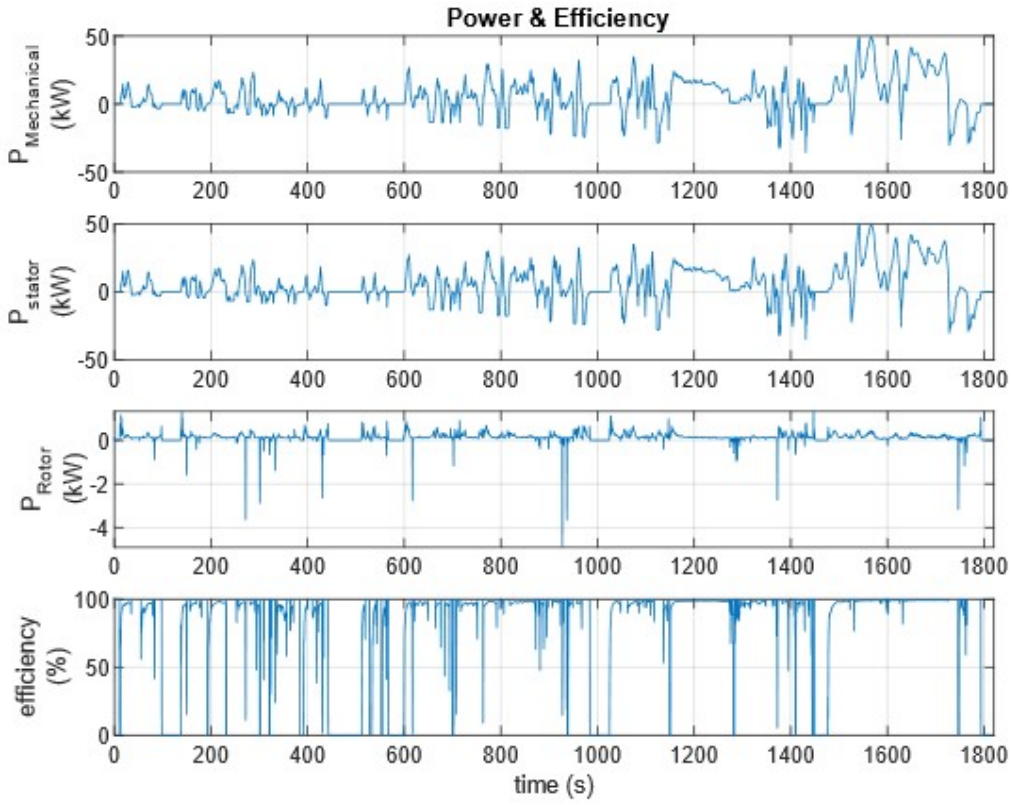

Figure 5.19: Instantaneous power and efficiency for WLTC drive cycle

5.3.3 Repeated acceleration profile

Repeated acceleration profile represented on T-ω envelop:

The repeated acceleration profile is a drive cycle that tests the machine over both the motor mode and regeneration mode at high speeds upwards of 7500 RPM. In Fig. 5.20, we see the repeated acceleration profile at 40% load (assuming all wheel drive with the front drive catering up to 40% of load). Thus, this drive cycle, as represented in T-ω envelop can be highlighted as shown in Fig. 5.21.

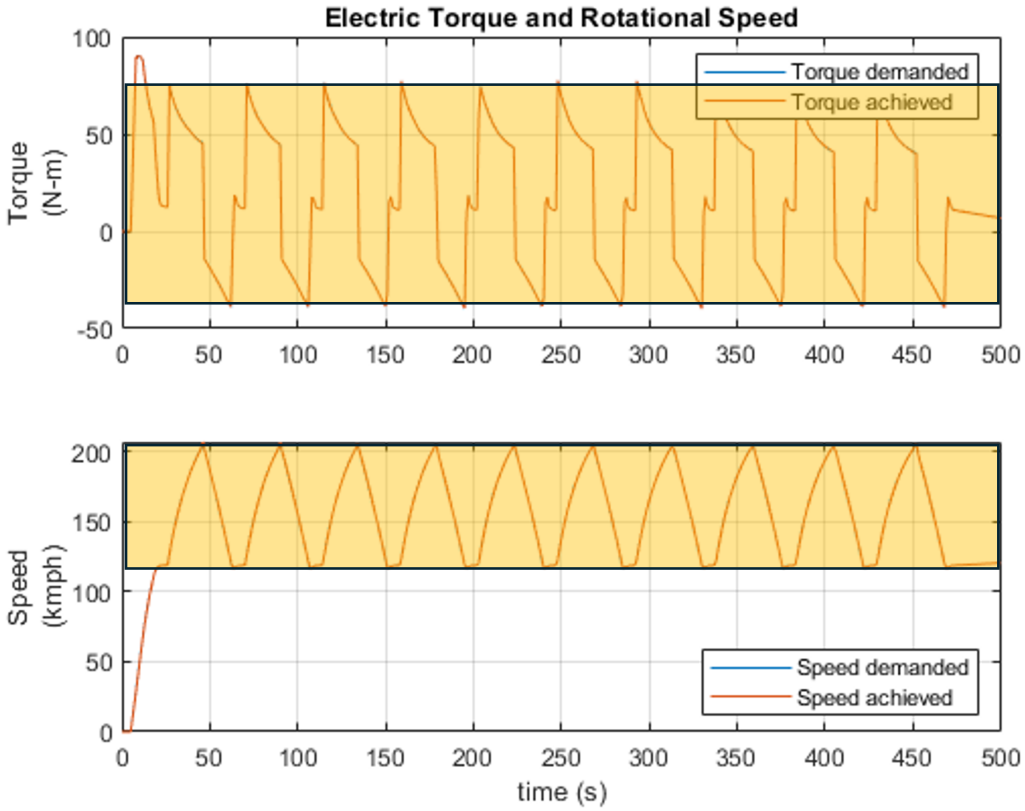

Figure 5.20: Repeated acceleration profile with 40% load assumption showing the compliance of torque and speed profiles achieved with the speed and torque profiles demanded

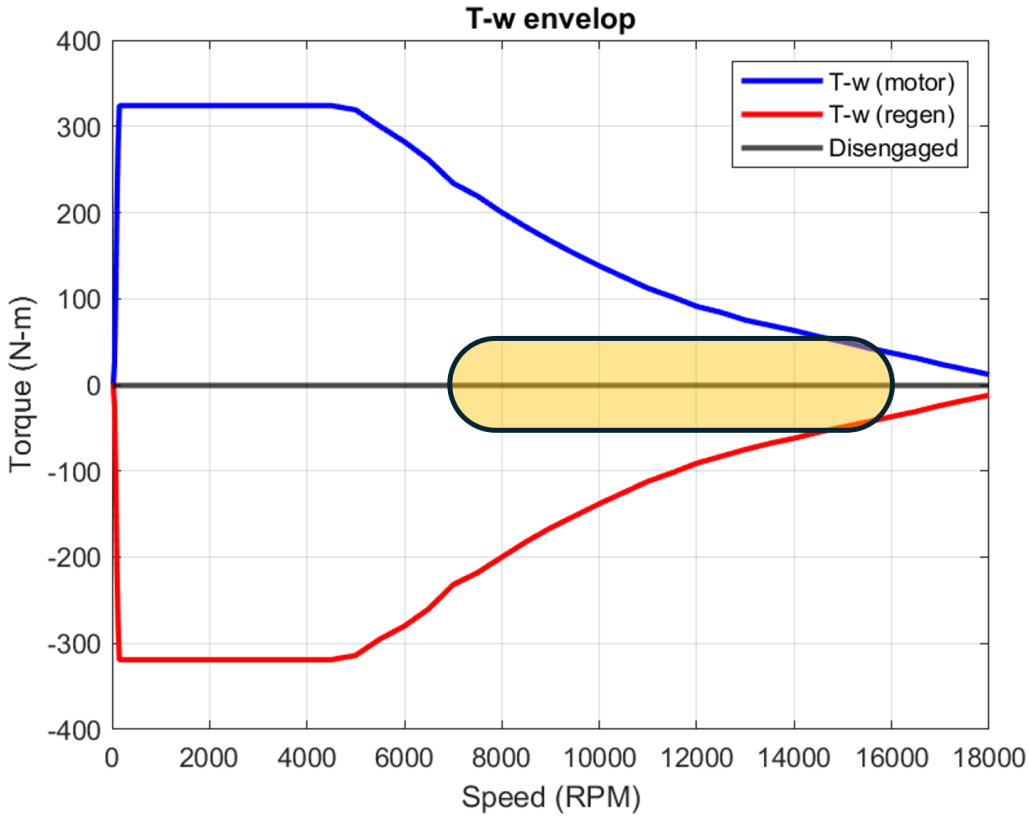

Figure 5.21: Representation of repeated acceleration drive cycle on the T vs ω plot

Voltage and Currents profiles:

The stator voltage is maxed out at 800 V (refer Fig. 5.22) since the speed profile is more than 120kmph (corresponding to the nominal speed). Thus this driving cycle can be considered as a special case that simulates in the field weakening zone of the T-ω envelop.

The rotor voltage on the other hand is under 35V for the whole drive cycle and has occasional spikes that reach up to 50V at the points where torque changes sign abruptly. This behaviour is as expected and very unlikely to be replicated in real-life driving scenarios. Hence, for all practical purposes, the rotor voltage requirements are within the stipulated power electronic requirements.

Similarly, the stator and rotor currents are also maintained well below the 70A and 30A respectively meeting the MOSFET current ratings followed per current industry conventions.

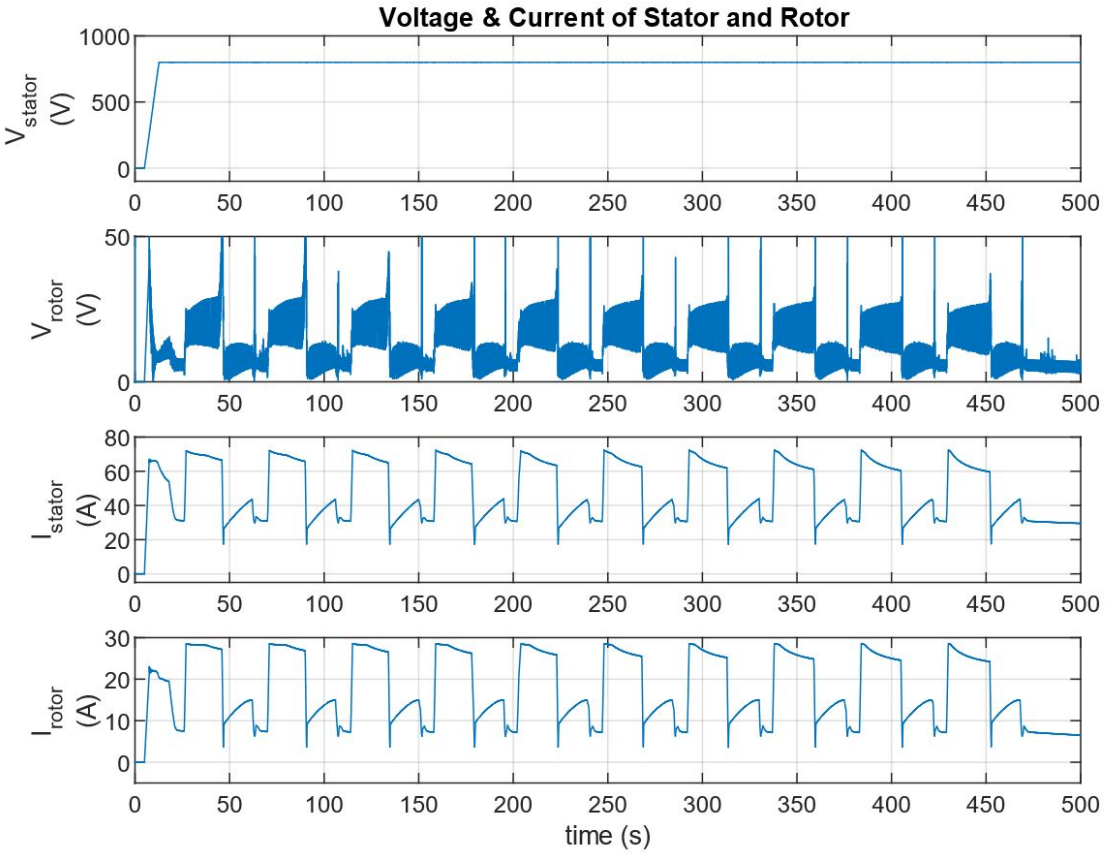

Figure 5.22: Voltage and current requirements at stator and rotor throughout the repeated acceleration drive cycle

Power and efficiency:

In Fig. 5.23, we see the variation of mechanical power, stator power and rotor power along with the instantaneous efficiency of the machine throughout the repeated acceleration profile. It can be seen that the rotor power requirement is under 1kW throughout the cycle with a few momentary exceptions which is less than 3% of the stator power. Also, the machine operates at efficiencies upwards of 98% throughout the duration of the cycle. This is in line with the steady state observations for the same torque speed combinations (refer Fig. 5.10).

As noted earlier, these calculations are made assuming ideal power electronics and so, these numbers may vary accordingly. It is also important to note that, these calculations would be more acceptable when done considering the state of health and state of charge of the batteries.

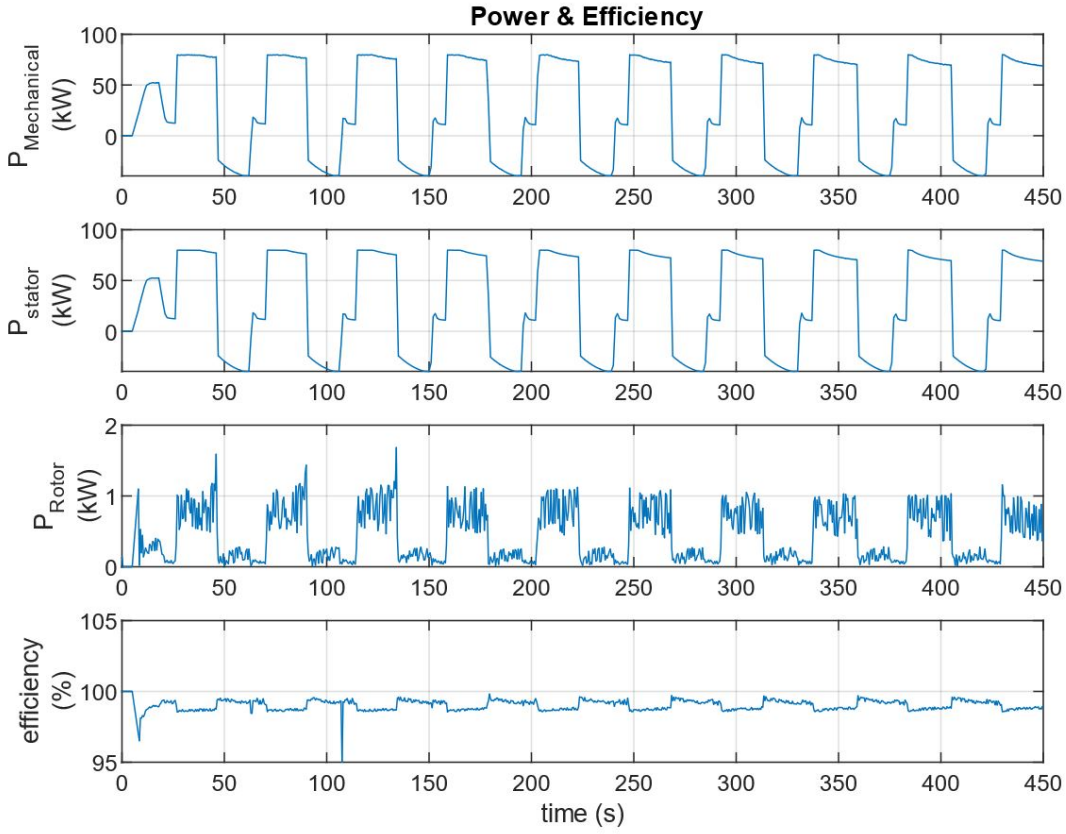

Figure 5.23: Instantaneous power and efficiency for repeated acceleration drive cycle (at 40% load)

6

Conclusion & Future Scope

6.1 Conclusion

In this thesis, the feasibility of implementing a Double Fed Induction Machine (DFIM) is explored in an automotive context, a novel approach previously unaddressed in existing literature. While DFIMs have been extensively studied in wind energy systems, their application in electric vehicles, particularly in an all-wheel-drive (AWD) setup, presented unique challenges and opportunities for innovation. The primary objective was to assess the viability of a DFIM-driven front axle combined with a PMSM on the rear axle, thereby creating an AWD system that leverages the strengths of both machine types.

The study began by examining the distinct configuration of the DFIM, which features windings on both the stator and rotor, unlike conventional induction machines. We initiated our research by reviewing the foundational principles of Doubly Fed Induction Generators (DFIGs) and their associated power electronics, which provided a basis for understanding the DFIM's behavior. Testing the DFIM as a standalone machine was a crucial step, allowing us to isolate and analyze its performance before integrating it into the full AWD system.

Throughout the research, one of the significant challenges was deciphering the 'IM with slip ring' model within the PLECS simulation environment. This required a substantial portion of the thesis to be dedicated to understanding the underlying model and accurately interpreting its outputs. Also, finalising the DFIM machine parameters was one of the challenging parts of the thesis. After going through the relevant literature, the machine parameters were decided based on the performance of the machine at various operating points. Once we gained a firm understanding of the DFIM's behavior, we systematically introduced additional components to test the machine's performance under various conditions, including steady-state and transient operations.

The results demonstrated that the DFIM could be effectively operated in an automotive context, particularly in scenarios where torque split and energy efficiency are critical. The key findings include the feasibility of a DFIM-based AWD system with fewer components compared to traditional systems, low rotor power requirements (1-3% of stator power), and the ability to operate in multiple modes, including synchronous, sub-synchronous, and super-synchronous. The efficiency mapping conducted as part of this study (refer Sec. 5.2) provides valuable insights into optimizing rotor excitation to achieve maximum efficiency across different torque and speed requirements.

However, the study also highlighted limitations, particularly the absence of a current controller in the finalized model. This omission prevented us from fully validating the DFIM's performance when integrated with the PMSM in a complete AWD system. Additionally, the simplified assump-

tions regarding machine losses, such as considering only resistive and inductive losses, suggest that real-world efficiency may differ from our findings.

6.2 Future Scope

The research presented in this thesis opens several avenues for future work. The immediate next step involves developing and implementing a current controller for the DFIM rotor. This will allow for more precise control of the machine and enhance its integration with the PMSM at the stator end. Additionally, future research should focus on the integration of power electronics, particularly the effects of battery state of charge and its impact on the DFIM's performance in real-world AWD scenarios.

Further investigation into the complete AWD system, including the interaction between the DFIM and PMSM, is essential for validating the theoretical findings presented in this thesis. This includes testing the system under various drive cycles and conditions that more accurately reflect typical automotive use cases. The inclusion of the PMSM controller at the stator end of the DFIM will be crucial in estimating the accurate efficiency of the DFIM and there could be opportunity to further improve the DFIM's performance and define better use cases.

Ultimately, this thesis contributes to the evolving understanding of DFIMs in the automotive industry, offering a foundational analysis that can inform future technological advancements in electric vehicle (EV) drivetrain systems. As the automotive industry continues to push towards more efficient and versatile electric powertrains, the insights gained from this research will be invaluable in guiding the development of next-generation AWD systems.

6.3 Sustainability

The introduction of the Double Fed Induction Machine (DFIM) in automotive applications has significant implications for sustainability and environmental impact. By reducing the number of components required in the drive system, the DFIM offers substantial cost savings for manufacturers, which not only enhances economic efficiency but also contributes to a more sustainable manufacturing process. Fewer components mean a reduction in material usage, energy consumption during production, and waste generation, all of which play a crucial role in minimizing the environmental footprint of automotive manufacturing.

Moreover, if this DFIM-based drive system is standardized across the industry, the potential for widespread sustainability benefits increases. The DFIM's capability to operate with low rotor power requirements and its versatility in different operational modes make it a compelling choice for future electric vehicles, where efficiency and resource optimization are paramount.

In summary, the adoption of DFIM technology in automotive systems not only offers economic benefits but also aligns with broader sustainability goals. By reducing component count, optimizing energy use, and exploring regenerative possibilities, the DFIM could play a pivotal role in the development of more sustainable and eco-friendly automotive ecosystems in the future.

Appendix A

Data

T_{regen} (N-m)	ω (RPM)	T_{motor} (N-m)	T_{regen} (N-m)	ω (RPM)	T_{motor} (N-m)
0	0	0	-232	7000	234
0	25	0	-218	7500	219
-25	50	25	-200	8000	200
-105	75	105	-182	8500	183
-210	100	210	-166	9000	167
-280	125	280	-152	9500	152
-319	150	324	-138	10000	138
-319	200	324	-125	10500	125
-319	300	324	-112	11000	112
-319	400	324	-102	11500	102
-319	500	324	-91	12000	91
-319	1000	324	-83	12500	84
-319	1500	324	-75	13000	75
-319	2000	324	-68	13500	69
-319	2500	324	-62	14000	63
-319	3000	324	-55	14500	56
-319	3500	324	-49	15000	50
-319	4000	324	-43	15500	43
-319	4500	324	-37	16000	37
-314	5000	319	-31	16500	31
-295	5500	300	-24	17000	24
-280	6000	282	-18	17500	18
-260	6500	261	-12	18000	12

Table A.1: Maximum torque (magnitude) achievable for different speeds in both motor and regen mode

Appendix B

Machine design

The flow chart below outlines the method to be adopted in order to further develop the machine in the subsequent procedure of this thesis topic.

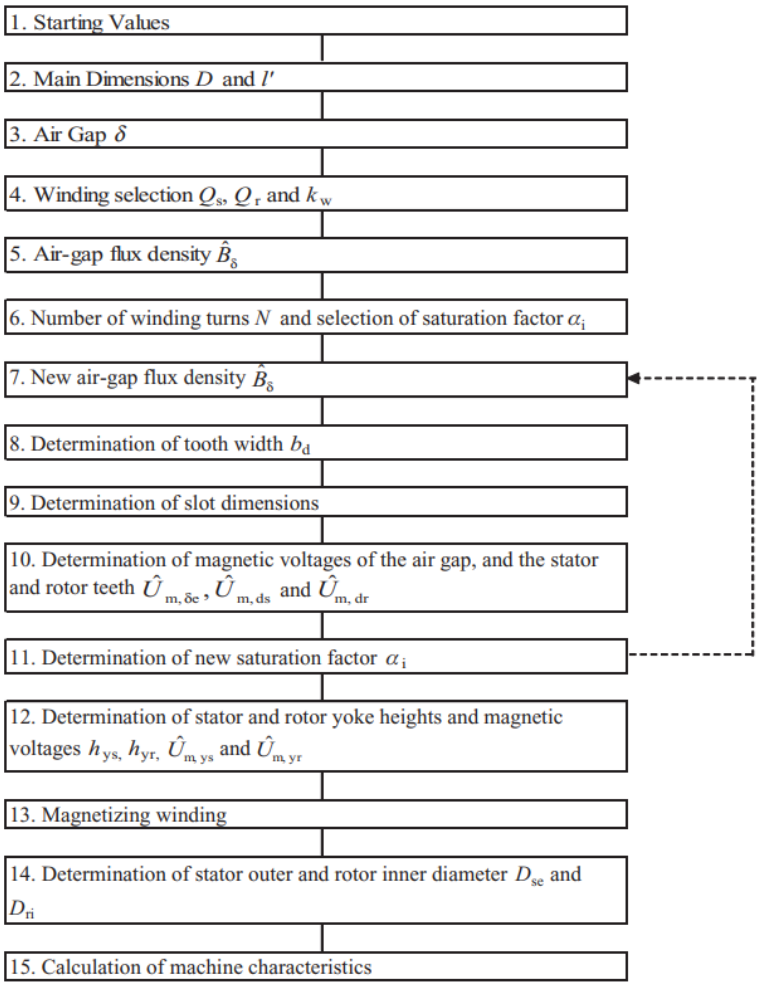

Figure B.1: Machine design process [21]

References

[1] G. Abad, J. Lopez, M. Rodriguez, L. Marroyo, and G. Iwanski. *Doubly fed induction machine: modeling and control for wind energy generation*. John Wiley & Sons, 2011.

[2] H. Abu-Rub, M. Malinowski, and K. Al-Haddad. *Power electronics for renewable energy systems, transportation and industrial applications*. John Wiley & Sons, 2014.

[3] B. Agrawal and M. K. Kirar. Comparative study for torque distribution between front rear drive in an all wheel drive electric vehicle. In *2023 IEEE Renewable Energy and Sustainable E-Mobility Conference (RESEM)*, pages 1–6, 2023. doi: 10.1109/RESEM57584.2023.10236042.

[4] B. Agrawal and M. K. Kirar. Comparative study for torque distribution between front & rear drive in an all wheel drive electric vehicle. In *2023 IEEE Renewable Energy and Sustainable E-Mobility Conference (RESEM)*, pages 1–6. IEEE, 2023.

[5] M. Bodson. Speed control for doubly fed induction motors with and without current feedback. *IEEE Transactions on control systems technology*, 28(3):898–907, 2019.

[6] F. Bonnet, P.-E. Vidal, and M. Pietrzak-David. Dual direct torque control of doubly fed induction machine. *IEEE Transactions on Industrial Electronics*, 54(5):2482–2490, 2007.

[7] F. BonnetFrancois, P.-E. Vidal, and M. Pietrzak-David. Dual direct torque control of doubly fed induction machine. *IEEE Transactions on Industrial Electronics*, 54(5):2482–2490, 2007. doi: 10.1109/TIE.2007.900330.

[8] R. Esterhuizen. *Comparative study between synchronous generator and doubly-fed induction generator in wind energy conversion systems*. PhD thesis, Tese, Cape Peninsula University of Technology, 2019.

[9] P. Han, M. Cheng, and Z. Chen. Dual-electrical-port control of cascaded doubly-fed induction machine for ev/hev applications. *IEEE Transactions on Industry Applications*, 53(2):1390–1398, 2016.

[10] P. Han, M. Cheng, and R. Luo. Design and analysis of a brushless doubly-fed induction machine with dual-stator structure. *IEEE Transactions on Energy Conversion*, 31(3):1132–1141, 2016.

[11] H. M. Hesar, H. A. Zarchi, G. A. Markadeh, and A. Khazaee. Maximum torque per total ampere strategy for vector-controlled brushless doubly fed induction machine drive taking iron loss into account. *IEEE Transactions on Power Electronics*, 37(11):13598–13605, 2022.

[12] G. Iwański, M. Piwek, and G. Dauksha. Doubly fed induction machine-based dc voltage generator with reduced oscillations of torque and output voltage. *Energies*, 16(2):814, 2023.

[13] Y. Liu and L. Xu. The dual-current-loop controlled doubly fed induction motor for ev/hev applications. *IEEE Transactions on Energy Conversion*, 28(4):1045–1052, 2013.

[14] D. C. Ludois, J. K. Reed, and K. Hanson. Capacitive power transfer for rotor field current in synchronous machines. *IEEE Transactions on Power Electronics*, 27(11):4638–4645, 2012.

[15] H. Mosaddegh Hesar, H. Abootorabi Zarchi, G. Arab Markadeh, and A. Khazaee. Maximum torque per total ampere strategy for vector-controlled brushless doubly fed induction machine drive taking iron loss into account. *IEEE Transactions on Power Electronics*, 37(11):13598–13605, 2022. doi: 10.1109/TPEL.2022.3183066.

[16] A.-T. Nguyen, B.-M. Nguyen, J. P. F. Trovao, and M. C. Ta. Modelling and control of dual-motor all-wheel drive electric vehicles using energetic macroscopic representation. In *Proceedings of the Canadian Society for Mechanical Engineering International Congress (CSME-CFD-SC2023)*, 2000.

[17] T.-T. Nguyen, H.-J. Yoo, and H.-M. Kim. A flywheel energy storage system based on a doubly fed induction machine and battery for microgrid control. *Energies*, 8(6):5074–5089, 2015.

[18] G. Peng, K. Ni, C. Gan, R. Qu, and Y. Hu. A direct starting method of doubly-fed induction machine for shipboard propulsion system application. In *2021 24th International Conference on Electrical Machines and Systems (ICEMS)*, pages 949–954. IEEE, 2021.

[19] A. Petersson. *Analysis, modeling and control of doubly-fed induction generators for wind turbines*. Chalmers Tekniska Hogskola (Sweden), 2005.

[20] G. Poddar and V. Ranganathan. Sensorless double-inverter-fed wound-rotor induction-machine drive. *IEEE Transactions on Industrial Electronics*, 53(1):86–95, 2006.

[21] J. Pyrhonen, T. Jokinen, and V. Hrabovcova. *Design of rotating electrical machines*. John Wiley & Sons, 2013.

[22] M. Ruviaro, F. Runcos, N. Sadowski, and I. M. Borges. Analysis and test results of a brushless doubly fed induction machine with rotary transformer. *IEEE Transactions on Industrial Electronics*, 59(6):2670–2677, 2011.

[23] C. Sadarangani et al. Brushless doubly-fed induction machine with rotating power electronic converter for wind power applications. In *2011 International Conference on Electrical Machines and Systems*, pages 1–6. IEEE, 2011.

[24] M. Vicatos and J. Tegopoulos. Steady state analysis of a doubly-fed induction generator under synchronous operation. *IEEE Transactions on Energy Conversion*, 4(3):495–501, 1989.

[25] M. Vicatos and J. Tegopoulos. Doubly-fed induction motor differential cascade. i. configuration and analysis in the steady state. *IEEE transactions on Energy Conversion*, 14(3):361–366, 1999.

[26] L. Xu, Y. Liu, and X. Wen. Comparison study of singly-fed electric machine with doubly-fed machine for ev/hev applications. In *2011 international conference on electrical machines and systems*, pages 1–5. IEEE, 2011.

[27] M. Zerzeri and A. Khedher. Optimal speed–torque control of doubly-fed induction motors: Analytical and graphical analysis. *Computers & Electrical Engineering*, 93:107258, 2021.

[28] M. Zerzeri, A. Khedher, and F. Jallali. Steady-state characteristics of dfim: the potentialities ofintegration in electrical traction systems. 2023.

DEPARTMENT OF SOME SUBJECT OR TECHNOLOGY
CHALMERS UNIVERSITY OF TECHNOLOGY
Gothenburg, Sweden
www.chalmers.se

CHALMERS
UNIVERSITY OF TECHNOLOGY